Separation and Purification Technology 281 (2022) 119811

Contents lists available at ScienceDirect

Separation and Purification Technology

journal homepage: www.elsevier.com/locate/seppur

MOF-based MMMs breaking the upper bounds of polymers for a large variety of gas separations☆

Hilal Daglar [a], Sena Aydin [b], Seda Keskin [a,*]

[a] Department of Chemical and Biological Engineering, Koc University, Rumelifeneri Yolu, Sariyer, 34450 Istanbul, Turkey
[b] Department of Computational Science and Engineering, Koc University, Rumelifeneri Yolu, Sariyer, 34450 Istanbul, Turkey

ARTICLE INFO

Keywords:
Mixed matrix membrane
Upper bound
Permeability
Selectivity
Gas separation

ABSTRACT

Mixed matrix membranes (MMMs) are a strong alternative to the conventional polymeric membranes which suffer from a trade-off between selectivity and gas permeability. Considering the existence of a large number of metal–organic frameworks (MOFs) and polymers, computational screening of MOF/polymer MMMs is strongly desired to explore their upper limits in various gas separation processes before experimental efforts. In this work, we computed permeability of CO_2, CH_4, N_2, O_2, H_2, and He gases in 5599 metal organic frameworks (MOFs) using atomically-detailed simulations and then assessed performances of >180,000 different MOF/polymer MMMs for 11 different gas separations He/H_2, He/N_2, He/CH_4, N_2/CH_4, H_2/N_2, H_2/CH_4 O_2/N_2, CO_2/N_2, CO_2/CH_4, H_2/CO_2, He/CO_2. Our results revealed that many MOF/polymer MMMs exceed the upper bounds due to their high gas permeability and/or selectivity. The impact of MOFs on the separation performances of polymers was examined to provide guidelines for the best MOF-polymer pairing for a variety of gas separations. Data showed that using MOFs as fillers significantly improves the permeability of CO_2, CH_4, N_2, O_2, H_2, and He gases in 41 different types of polymers without changing their selectivities. Many MOFs offer a great opportunity for MMM applications by improving both the permeability and selectivity of polymers such as of Teflon AF-2400 for N_2/CH_4, PTMSP-co(95/5) for H_2/CH_4, PTMSDPA for O_2/N_2 and PTMSP for CO_2/CH_4 separations. The best MOF fillers leading to MMMs with exceptional selectivities were found to have narrow pores and low porosities. These results will contribute to directing the experimental efforts to the best MOF/polymer MMM materials for numerous industrially important gas separation applications.

1. Introduction

Gas separation applications play a crucial role in today's energy production and chemical purification industries such as hydrogen purification. In today's technology, cryogenic distillation (e.g. for helium purification), adsorption-based gas separation using pressure swing adsorption (PSA) (e.g. for natural gas purification) and temperature swing adsorption (TSA), chemical absorption using ammonia dominate the industrial gas separation methods. The 10–15% of the world's total energy are consumed for these gas separation processes [1]. Therefore, they are highly expensive and energy intensive. Compared to these conventional separation technologies, membrane-based gas separation is environmentally safe with advantages of requiring low energy consumption and being easy to scale up [2]. Polymers offer easy processability, large-scale operation, and excellent mechanical properties in membrane-based gas separation processes, but they have a trade-off between gas permeability and selectivity [3]. When a polymeric membrane has high permeability, it generally suffers from low selectivity or vice versa, which have led to the definition of upper bounds for gas separation performances of polymers [4,5]. Incorporation of high-performance inorganic fillers into polymers to obtain mixed matrix membranes (MMMs) has become an important path in overcoming the selectivity-permeability trade-off [6–8]. Different types of materials such as activated carbons, silica, and zeolites have been widely used as fillers in polymers to generate MMMs and these MMMs have been reported to exhibit generally higher separation performances compared to pure polymers [9–11]. Metal organic frameworks (MOFs) are promising filler materials due to their high porosities, high surface areas, and structural tunabilities [12]. MOF/polymer MMMs have been studied for different gas separation applications and using MOFs as fillers in polymers generally improves the gas permeability and membrane selectivity

☆ Submitted to *Separation and Purification Technology*.

* Corresponding author.
E-mail address: skeskin@ku.edu.tr (S. Keskin).

https://doi.org/10.1016/j.seppur.2021.119811
Received 28 August 2021; Received in revised form 20 September 2021; Accepted 22 September 2021
Available online 1 October 2021
1383-5866/© 2021 The Author(s). Published by Elsevier B.V. This is an open access article under the CC BY-NC-ND license (http://creativecommons.org/licenses/by-nc-nd/4.0/).

Nomenclature

Notations and Abbreviations Parameters

MOF	Metal-organic framework
MMM	Mixed matrix membrane
LCD	The largest cavity diameter (Å)
PLD	Pore limiting diameter (Å)
S_{acc}	Accessible surface area (m^2/g)
D_i	Self-diffusion coefficient of gas species i (m^2/s)
c_i	Adsorbed gas loading for species i (mol/m^3)
f_i	Feed side partial pressure of the gas species i (Pa)
N_i	Amount of adsorbed gas loading for species i (mol/kg)
ϕ	Volume fraction of MOF fillers in the polymer matrix
P_i^{MOF}	Gas permeability of MOFs (for the gas species i) (Barrer)
P_i^{MMM}	Gas permeability of MMM (for the gas species i) (Barrer)
P_i^{P}	Gas permeability of polymer (for the gas species i) (Barrer)
$S_{mem.i/j}^{MOF}$	Membrane selectivity of MOF filler
$S_{i/j}^{MMM}$	Membrane selectivity of MMM
$S_{ads.i/j}^{MOF}$	Adsorption selectivity of MOF
$S_{diff.i/j}^{MOF}$	Diffusion selectivity of MOF
PTMSP	Poly[1-(trimethylsilyl)-1-propyne]
PIM	Polymers of intrinsic microporosity
TABH	1,2,4,5-Tetraaminobenzene tetrahydrochloride
ODA	4,4′- oxydianiline
PTMGP	Poly(1-trimethylgermyl-1-propyne)
MEEP	Poly-(bis((methoxyethoxy)ethoxy)phosphazene)
PDPA	Poly(diphenyl acetylene)
PI	Polyimide
DSDA	3,3′,4,4′-diphenylsulfonetetracarboxylic dianhydride
DDBT	3,7-diamino-2,8(6)-dimethyldibenzothiophene sulfone
6FDA	4,4′-(hexafluoroisopropylidene)diphthalic anhydride
PMDA	Pyromellitic anhydride
TADATO-4A	Thianthrene-2,3,7,8-tetracarboxylic acid-5,5,10,10-tetraoxide
PTMSDPA	Poly[1-phenyl-2-(4-trimethylsilyl)phenylacetylene]
PPO	Poly(2,6-dimethyl-l,4-phenyl oxide)
6FDA-6FpDA	Hybrid materials based upon a 6FDA-6FpDA polyimide
DABA	3,5-Diamino benzoic acid
BPDA	3,3′,4,4′-Biphenyltetracarboxylic dianhydride
Hyflon AD	Amorphous fluoropolymer prepared from 80 mol% 2,2,4-trifluoro-5-trifluoromethoxy-1,3-dioxole (TTD) and 20 mol% tetrafluoroethylene (TFE), commercially known as Hyflon AD 80
HBA	4-hydroxybenzoic acid
HNA	2-hydroxy-6-naphthoic acid
Polyimide (NTDA-BAPHFDS(H))	Protonated form of 1,4,5,8-naphthalene tetracarboxylic dianhydride-2,2-bis[4-(4-aminophenoxy)phenyl] hexafluoro propane disulfonic acid
6FDA-DIA	Cross-linked N,N′-dipropargyl (4–4′-hexafluoroisopropylidene) bisphthalimide polyimide
PBOI-2-Cu+	Polybenzoxazinone imide
6FDA-mPDA	4,4′-(hexafluoroisopropylidene)diphthalic dianhydride-m-phenylenediamine

of polymers [13–15]. MOF-based MMMs are widely synthesized using different techniques such as one-pot synthesis [16] and tested for many different gas separation applications [17–19]. Recently, Smith's group published an extensive review article, listed the experimental gas separation performances of different MOF/polymer MMMs and addressed the efforts and importance of using predictive permeation models to compute the gas separation performances of MMMs [15]. Experimental studies have generally focused on a small number and type of MOFs and polymers to test the separation potential of MOF/polymer MMMs for a specific gas separation application. Considering the large number and variety of MOFs existing in the Cambridge Structural Database (CSD) [20], it is not possible to experimentally test all the possible MOF-polymer combinations for a large variety of gas separations.

High-throughput computational screening studies play a critical role in identifying the best MOF/polymer MMMs for a target gas separation. For example, 3794 MOFs were screened using molecular simulations to select the best MOF fillers and 64 MOF/polymer MMMs composed of the top 8 best performing MOFs and 8 polymers were examined in detail [21]. Results revealed that CO_2 permeabilities of all polymers were improved while CO_2/CH_4 selectivities of some polymers increased by the incorporation of MOFs into the polymers. CO_2/CH_4 separation performances of 116 MMMs obtained from 29 different covalent organic frameworks (COFs) and 4 polymers were studied using molecular simulations and results showed that COF fillers enhanced the CO_2 permeability and CO_2/CH_4 selectivity of several polymers [22]. H_2/N_2 separation performances of 3765 MOFs were computed to identify the best MOF fillers, and 13 MOFs having high H_2 permeability and high H_2/N_2 selectivity were incorporated into 8 polymers [23]. While H_2 permeabilities of the majority of MMMs were approximately two times higher than those of pure polymers, H_2/N_2 selectivities of a small number of MMMs were higher compared to polymers.

CO_2/N_2 separation performances of MOF/polymer MMMs were studied to predict the cost of carbon capture with respect to MMMs' selectivity and it was shown that there are many MOF/polymer MMMs yielding carbon capture with less than $50 for one tonne CO_2 removal [24]. We computed CO_2 permeabilities and CO_2/N_2 selectivities of 109,508 MMMs composed of 7822 MOFs and 14 polymers in our previous work [25] and results showed that incorporating MOFs into polymers almost doubled the CO_2/N_2 selectivity of the polymers. O_2/N_2 separation performances of 78,806 different types of MOF/polymer MMMs were reported to describe the upper limits of O_2 permeabilities and O_2/N_2 selectivities of MOF/polymer MMMs [26]. As can be seen from this literature review, most of the computational studies focused on CO_2/N_2 and CO_2/CH_4 separations, whereas many other industrially important gas separations such as N_2/CH_4, He/N_2, He/CH_4, He/CO_2, He/H_2, H_2/CO_2, H_2/CH_4 have been overlooked. Therefore, we still do not know the separation potential of many MOF-polymer combinations for different types of separations. A MOF/polymer MMM exhibiting low gas selectivity for a specific gas separation may have high performance for another separation. Thus, computational efforts examining a large number of MOFs and polymers for a variety of gas separations are highly required to describe the upper performance limits of MOF/polymer MMMs.

In this study, we focused on the most commonly studied gases, CO_2, CH_4, N_2, O_2, H_2, He, and used atomically-detailed simulations to compute the gas permeability and selectivity of MOF/polymer MMMs for 11 different gas separations including He/H_2, He/N_2, He/CH_4, N_2/CH_4, H_2/N_2, H_2/CH_4, O_2/N_2, CO_2/N_2, CO_2/CH_4, H_2/CO_2, He/CO_2. Grand canonical Monte Carlo (GCMC) and molecular dynamics (MD) simulations were performed to compute single-component gas adsorption and diffusion data of 5599 different types of MOFs and this data was used to assess permeabilities of CO_2, CH_4, N_2, O_2, H_2, and He gases in MOFs. We then computed the gas permeability and selectivity of a total of 181,249 different types of MOF/polymer MMMs for all the gas separations listed above and compared them with the separation performances of the experimentally reported MMMs in the literature. Our results for a very large number of MOF/polymer MMMs revealed how using different types of MOF fillers in polymers change the upper

performance limits of polymeric membranes depending on the gas separation. A guideline representing the best MOF-polymer matching for each gas separation of interest was provided together with the detailed analysis of relationship between structural properties of MOFs and selectivities of MMMs. Overall, the important contributions of this work can be summarized as follows: (i) Gas separation potentials of many new MOFs which have never been studied as fillers in MMMs before were reported. (ii) Performances of MOF/polymer MMMs were investigated for a large variety of separations, 11 different separation applications, He/H_2, He/N_2, He/CH_4, H_2/CH_4, H_2/CO_2, N_2/CH_4, H_2/N_2, O_2/N_2, CO_2/N_2, CO_2/CH_4 and He/CO_2. (iii) Molecular simulations were performed at realistic conditions for single-component gases, in accordance with the existing data of polymeric membranes. (iv) Guidelines were provided for the first time to match polymers with MOFs for each gas separation and structural properties of MOFs that lead to high performance MMMs were revealed. We believe that our results will contribute into directing the extensive experimental efforts for the design and development of high-performance MOF/polymer MMMs for a large variety of industrially important gas separations.

2. Computational details

We started with the most recent computation-ready, experimental (CoRE) MOF database including over 12,000 materials [27] so all the MOFs we studied are already synthesized. Zeo++ was used to compute the structural properties of MOFs such as the largest cavity diameter (LCD), pore limiting diameter (PLD), accessible surface area (S_{acc}) and porosity as described in our previous work [26]. We only considered the MOFs with $S_{acc}>0$ m^2/g. To allow the permeation of all gases through the pores, we eliminated the MOFs with PLDs smaller than the size of the largest gas molecule (3.73 Å) studied, which is CH_4 in this work. Since the initial states of the MD simulations (loading and positions of the gas molecules) were taken from the GCMC simulations, MD simulations were performed only for MOFs having gas uptakes of at least 1 molecule/unit cell of structure. After obtaining the MD simulation results, we only selected the MOF having gas diffusivities higher than the limit value ($>10^{-8}$ cm^2/s) to characterize molecular diffusion. After all these eliminations, we ended up with 864 MOFs for computing permeability of He, 2124 MOFs for CO_2, 3255 MOFs for H_2, and 5599 MOFs for CH_4, O_2 and N_2 gases.

First, gas uptakes of MOFs (N_i^{MOF}) were computed at 1 bar, 298 K, then the results of the GCMC simulations were used to compute the self-diffusivity (D_i^{MOF}) of gases at their adsorbed loadings using MD simulations. We used the RASPA software to perform all molecular simulations [28]. MOF-gas and gas–gas intermolecular interactions which include repulsion-dispersion forces and electrostatic interactions were described with Lennard-Jones 12–6 (LJ) and Coulomb potentials, respectively. The LJ potential parameters of framework atoms were taken from a generic force field, the universal force field (UFF) [29]. The force field used in molecular simulations can affect the predicted gas separation performances of the materials. Demir et al. [30] compared the gas uptakes obtained with different density functional theory (DFT) based-force fields and UFF with experimental results for six MOFs and showed that the performance of UFF to predict experimental results is similar to the DFT-based force field and simulation results obtained with UFF give a good agreement with experimental results in most of the cases. Watanabe et al. [31] discussed the applicability of generic force fields to MOFs with four representative studies [32–35] and concluded that generic force fields such as UFF give reasonable results in high-throughput screening studies but must be used with caution when predicting the separation performance of an individual MOF, since specific interactions can exist such as between CO_2 and open metal sites of MOFs [36]. The applicability of UFF for material screening was also tested by McDaniel et al. [37] and results showed that although predictions with UFF for CO_2 uptake were considerably different from those predicted with a more accurate *ab initio* force field, the ranking of MOFs based on the CO_2 uptakes was similar. We also showed in Fig. S1 that the gas permeability of MMMs obtained from simulations using UFF agree well with the experimentally measured ones. To estimate the partial atomic charges of MOFs, the charge equilibration method (Qeq) [38] as implemented in the RASPA was used and to calculate long range electrostatic interactions, the Ewald summation was used [39]. CH_4 [40], He [40], and H_2 [41] were represented as nonpolar, single, and spherical atoms. O_2 [42] and N_2 [43] were modelled as three-site molecules including a dummy atom as the center of mass and two sites with O or N atoms. CO_2 [44] was also modeled as linear and three-site rigid molecule. N_2, O_2 and CO_2 have quadrupole moments, thus the electrostatic interactions between these gas molecules and MOF atoms were considered. Neglecting these interactions can significantly underestimate the gas adsorption and hence gas separation performances of MOFs [45]. The LJ potentials and partial point charges of gases were provided in Table S1 of Supporting Information (SI).

We first performed GCMC simulations to obtain gas uptake using the first 2×10^4 cycles for initialization and the last 2×10^4 (5×10^4) cycles for taking the ensemble averages for the adsorption of CH_4, H_2, and He (CO_2) gases. To compute O_2 and N_2 adsorption, we followed the same GCMC procedure as reported in our recent study [26]. MD simulations were performed in NVT ensemble using a step size of 1 fs up to a total of 5 ns at 298 K. Nose-Hoover thermostat [46] was used to keep the temperature constant. In each MOF, MD simulations were run for 5×10^6 cycles with 10^3 cycles for initialization and 10^4 cycles for the equilibration. We computed the self-diffusivity (D_i) of each gas by using the slope of the mean square displacement (MSD) of gas molecules with respect to time, following the Einstein's relation [39]. More detailed information about simulations can be found in our previous studies [25,26].

Using the single-component gas adsorption and diffusion data, adsorption selectivities ($S_{ads,i/j}^{MOF} = N_i^{MOF}/N_j^{MOF}$) and diffusion selectivities ($S_{diff,i/j}^{MOF} = D_i^{MOF}/D_j^{MOF}$) of MOFs were computed, respectively. Here, N is the amount of adsorbed gas loading (mol/kg) and D is the self-diffusion coefficient (m^2/s) for gases, i and j. Single-component gas permeabilities (P_i^{MOF}) through MOFs were calculated by $P_i^{MOF} = c_i^{MOF} \times D_i^{MOF}/f_i$ where c_i, D_i, and f_i are the adsorbed gas loading (mol/m^3), self-diffusion coefficient of gas (m^2/s) and feed side partial pressure of the gas (Pa), respectively. To calculate P_i^{MOF}, feed side pressure was assumed to be at 1 bar and permeate side was assumed to be under vacuum. We note that all molecular simulations were performed on ideal MOF crystals without defining a membrane thickness. Membrane selectivities of MOFs were computed as the ratio of single-component gas permeabilities, $S_{mem,i/j}^{MOF} = P_i^{MOF}/P_j^{MOF}$. All the selectivities that we reported in this study are ideal selectivities calculated based on single-component data.

For studying MOF/polymer MMMs, we focused on 11 different gas separations, He/H_2, He/N_2, He/CH_4, N_2/CH_4, H_2/N_2, H_2/CH_4, O_2/N_2, CO_2/N_2, CO_2/CH_4, H_2/CO_2, He/CO_2. Different types of polymers have been tested for these gas separations and their permeability/selectivity values are already available in the literature. We specifically selected 41 different polymers focusing on the polymers which defined the Robeson's upper bound [4] for each gas separation. The names, experimentally reported membrane selectivities ($S_{mem,i/j}^{P}$), and gas permeabilities (P_i^P) of these polymers for 11 different gas separations were listed in Tables S2-S12. Predicting the separation performances of MOF/polymer MMMs by using a theoretical permeation model was first reported by Keskin and Sholl [47]. The good agreement between model predictions and the experimental permeation data is shown for IRMOF-1/Matrimid MMM, indicating the validity of this methodology. To predict gas permeabilities of MMMs, we used the Maxwell model [48] through which simulated gas permeability data of MOFs and experimentally measured gas permeability data of polymers were combined as follows:

$$P_i^{MMM} = P_i^P \times \left[\frac{2 \times (1-\phi) + (1+2\phi) \times \left(P_i^{MOF}/P_i^P\right)}{(2+\phi) + (1-\phi) \times \left(P_i^{MOF}/P_i^P\right)} \right]$$

Here P_i^{MMM} is the gas permeability of MMM, P_i^{MOF} is the gas permeability of MOF filler, P_i^P is the gas permeability of polymer for the gas species i, and ϕ is the volume fraction of MOF fillers in the polymer matrix, used as 0.2 throughout this study. Selectivities of these MMMs ($S_{i/j}^{MMM}$) were calculated as the ratio of gas permeabilities: $S_{i/j}^{MMM} = P_i^{MMM}/P_j^{MMM}$. Our computational methodology was shown in Scheme S1 of SI.

There can be deviations between the simulated and experimental results due to several reasons. In our molecular simulations, we assumed rigid frameworks, defect-free crystalline structures and used a generic force field to define the interactions between the gas molecules and a large diversity of MOFs. These assumptions may not be valid for all MOFs. Considering structural flexibility of MOFs, representing the defects in structures, and using force fields that are specifically produced for each MOF by quantum-based methods might increase the accuracy of simulations, but these are of course not possible when thousands of MOFs were simulated in a screening study. We first showed the comparison of the permeability data of MMMs for various gases reported in our previous works [26,49–51] with the experimental data reported in the literature in Fig. S1(a). We note that molecular simulations were performed at the same pressure, temperature, and using the same filler loading with the corresponding experiments. Fig. S1(a) includes 93 data for MMMs composed of 9 different common MOFs (MIL-101, MIL-53, ZIF-8, IRMOF-1, CuBTC, UiO-66, ZIF-90, CuTPA, ZIF-71) and 10 different polymers (PSF, Matrimid, PPEES, Ultem, 6FDA-ODA, ODPA-TMA, PU, 6FDA-DAM, 6FDA-Durane, PVAc). The names of the MMMs and filler loadings are provided in Table S13. Fig. S1(a) showed that there is a good agreement between the predictions and experiments for O_2, N_2, CH_4, H_2 and CO_2 permeabilities of MMMs. We also compared the predicted gas permeabilities of MMMs (molecular simulations were performed at 1 bar, 298 K) including MOF fillers available in our MOF subset with experimental data as reported in Table S14. Simulated gas permeabilities of MMMs for O_2, He, CH_4, H_2, and N_2 agree well with the experimental ones in Fig. S1(b). Motivated from these agreements, we applied the same approach to compute the gas permeability of 1884 MMMs for He/CO_2, 3456 MMMs for He/CH_4, 3582 MMMs for H_2/CO_2, 6048 MMMs for He/N_2, 6768 MMMs for He/H_2, 10,620 MMMs for CO_2/N_2, 16,992 MMMs for CO_2/CH_4, 19,530 MMMs for H_2/CH_4, 22,785 MMMs for H_2/N_2, 44,792 MMMs for O_2/N_2, and 44,792 MMMs for N_2/CH_4 separation. Overall, we examined the largest number of MMMs (181,249 in total) composed of experimentally synthesized MOFs reported to date.

3. Results and discussions

3.1. Adsorption and diffusion of gases in MOFs

Gas adsorption and diffusion properties are the key factors to compute gas separation performances of MOFs. We first examined the uptakes and self-diffusion coefficients of He, H_2, CH_4, CO_2, N_2 and O_2 in MOFs. Fig. 1(a) shows that He (6.84×10^{-3}–0.3 mol/kg) and H_2 (6.77×10^{-3}–0.34 mol/kg) are the two gases with the lowest uptakes. The LJ energy parameters for He (ε/k_B:10.9 K) and H_2 (ε/k_B:34.2 K) are lower compared to those of other gas molecules which reflects the weak dispersion interactions of He and H_2 with MOFs. The highest gas uptakes (0.12–27.5 mol/kg) were obtained for CO_2 since it has three interaction sites and high quadrupolar moment [52] leading to electrostatic interactions in addition to the dispersion interactions. Overall, Fig. 1(a) demonstrated that the range of gas uptakes in MOFs follows the order of $CO_2 > CH_4 > N_2 > O_2 > H_2 > He$.

There is an inverse relation between adsorption and diffusion properties of gases. Fig. 1(b) shows the range of the self-diffusivities of gases

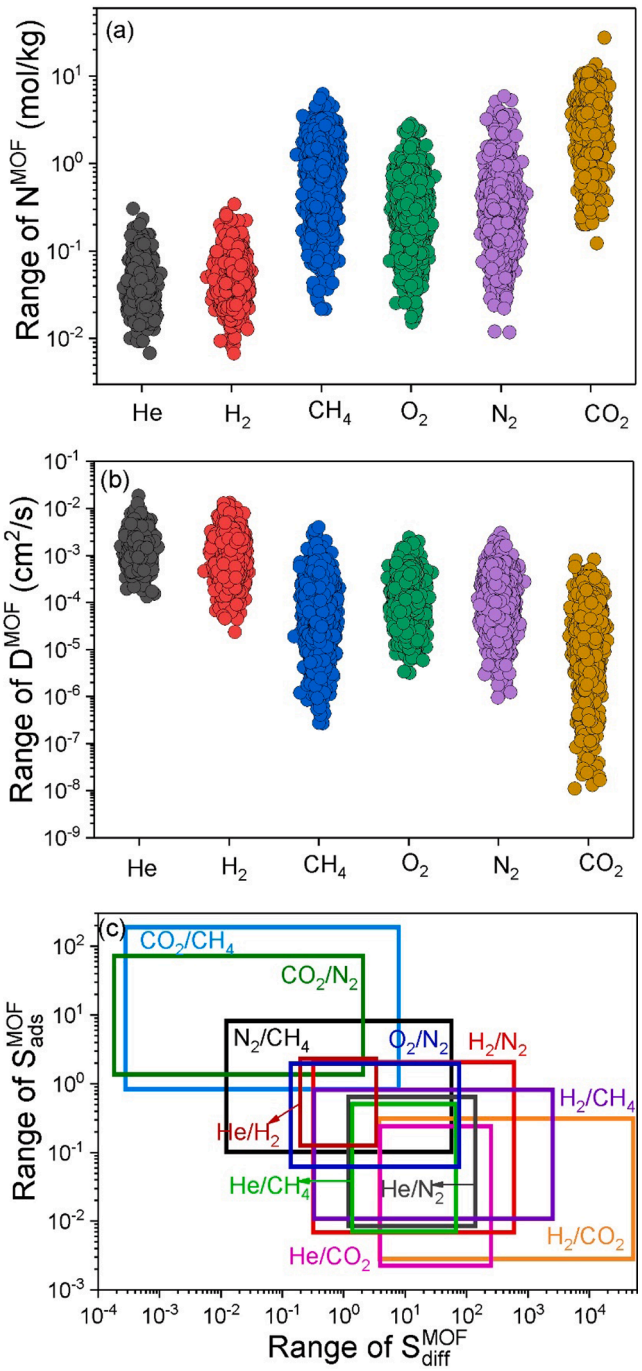


Fig. 1. Computed (a) adsorption and (b) diffusion properties of He, H_2, CH_4, O_2, N_2 and CO_2 gases in MOFs. (c) The range of adsorption and diffusion selectivities of MOFs for 11 different gas separations. The corners of the rectangles represent the maximum and minimum adsorption and diffusion selectivities of MOFs for gas separations.

follow the order of He > H_2 > CH_4 > O_2 > N_2 > CO_2. Weakly adsorbed gas molecules generally diffuse faster than the strongly adsorbed ones. For example, diffusion coefficients of He (1.36×10^{-4}–1.87×10^{-2} cm^2/s) and H_2 (1.24×10^{-5}–1.31×10^{-2} cm^2/s) are the highest as expected since they are weakly adsorbed and lighter. CH_4 (2.75×10^{-7}–4.02×10^{-3} cm^2/s), N_2 (9.47×10^{-7}–3.01×10^{-3} cm^2/s) and O_2 (3.18×10^{-6}–2.41×10^{-3} cm^2/s) diffuse slower compared to He and H_2. This can be explained with the stronger MOF-gas interactions and higher molecular weights of CH_4, N_2, and O_2 compared to H_2 and He. Diffusion coefficients of CO_2 in MOFs were calculated to be in a wide range ($1.10 \times$

10^{-8}–8.16 × 10^{-4} cm^2/s), which includes the lowest self-diffusivity among those computed for all gas molecules. This can be attributed to the very strong adsorption of CO_2 in some MOFs.

Using the adsorption and diffusion data of gases, we computed S_{ads}^{MOF} and S_{diff}^{MOF} for 11 different gas separations in Fig. 1(c). The maximum achievable S_{ads}^{MOF}values for He/CO_2, H_2/CO_2, He/CH_4, He/N_2, H_2/CH_4, H_2/N_2, O_2/N_2, He/H_2, N_2/CH_4, CO_2/N_2 and CO_2/CH_4 were reported as 0.25, 0.3, 0.5, 0.65, 0.8, 2.0, 2.0, 2.3, 7.9, 67 and 180, respectively. On the other hand, S_{diff}^{MOF} values for CO_2/N_2, He/H_2, CO_2/CH_4, N_2/CH_4, He/CH_4, O_2/N_2, He/N_2, He/CO_2, H_2/N_2, H_2/CH_4 and H_2/CO_2 were reported as 1.8, 3.7, 8.3, 58, 61, 75, 143, 234, 593, 2.42 × 10^3, and 4.9 × 10^4 respectively. Adsorption generally favors one gas while diffusion favors the other gas in a given pair. For example, due to stronger adsorption of N_2 compared to He, the range of He/N_2 adsorption selectivity is lower than 1 (8.27 × 10^{-3}–0.65), while He/N_2 diffusion selectivity is higher than unity (1.5–143) because of the faster diffusion of He compared to N_2. For N_2/CH_4 separation, the range of self-diffusivity of CH_4 (2.75 × 10^{-7}–4.02 × 10^{-3} cm^2/s) is similar to that of N_2 (9.47 × 10^{-7}-3.01 × 10^{-3} cm^2/s) and the range of CH_4 uptake (0.02–6.3 mol/kg) is also similar to that of N_2 uptake (0.04–5.9 mol/kg). However, for most MOFs (4599), adsorption generally favors one gas (CH_4 for most cases) while diffusion favors the other gas (N_2 for most cases). After calculating gas permeabilities, we obtained both CH_4 (4959) and N_2 (640) selective MOFs. Therefore, both competitive adsorption (thermodynamic separation) and differences in diffusivity (kinetic separation) play a role on the separation mechanism for N_2/CH_4 separation. We also note that studies reveal structural properties such as PLD and pore size distribution of MOFs are important parameters to separate N_2 from CH_4 [53]. In CO_2 related gas separations, such as CO_2/N_2 and CO_2/CH_4, MOFs exhibit a large range of diffusion selectivity compared to adsorption selectivity. For example, S_{diff}^{MOF} for CO_2/N_2 varies between 2.07 × 10^{-4}–1.8, significantly larger than the range of S_{ads}^{MOF} (1.5–67). This can be explained with the existence of MOFs in which very low CO_2 diffusivities (~10^{-8} cm^2/s) were observed as shown in Fig. S2. The MOFs in which CO_2 molecules have a low self-diffusion coefficient (<10^{-6} cm^2/s) adsorb high amount of CO_2 (>2 mol/kg) in their small pores. When CO_2 molecules strongly adsorb in the small pores of MOFs, diffusion of CO_2 becomes slow, resulting in very low CO_2/N_2 diffusion selectivity. Using this adsorption and diffusion data of gases in MOFs, permeability and selectivity of MOF and MOF/polymer membranes were calculated.

3.2. Separation performances of MOFs and MOF/polymer MMMs

In this section, we examined the gas permeability and selectivity of MOFs and MOF/polymer MMMs for natural gas purification (N_2/CH_4, CO_2/CH_4), flue gas separation (CO_2/N_2), air separation (O_2/N_2), H_2 purification (H_2/N_2, H_2/CH_4, H_2/CO_2), and He purification (He/H_2, He/N_2, He/CH_4, and He/CO_2). Purification of the natural gas, for which the main component is CH_4, with high efficiency is strongly desired for energy-intensive industrial processes [54]. Since the main impurities in natural gas sources are N_2 and CO_2, membrane materials with good N_2/CH_4 and CO_2/CH_4 separation performances are needed. N_2/CH_4 selectivities of polymeric membranes are generally low (1.3–4.4) as shown in Table S9 due to the similar kinetic diameters of N_2 and CH_4 molecules. Thus, using MOF structures having a large diversity of pore sizes may offer an opportunity to separate these molecules. N_2 permeability and N_2/CH_4 selectivity of 5599 MOFs are shown in Fig. 2(a). MOFs were found to have a large range of N_2 permeabilities (1.33 × 10^3–6.21 × 10^6 Barrers) and N_2/CH_4 selectivities (2.9 × 10^{-2}–27). We extended the upper bound with a dashed line in Fig. 2(a) because the gas permeabilities of MOFs were computed to be significantly higher than the

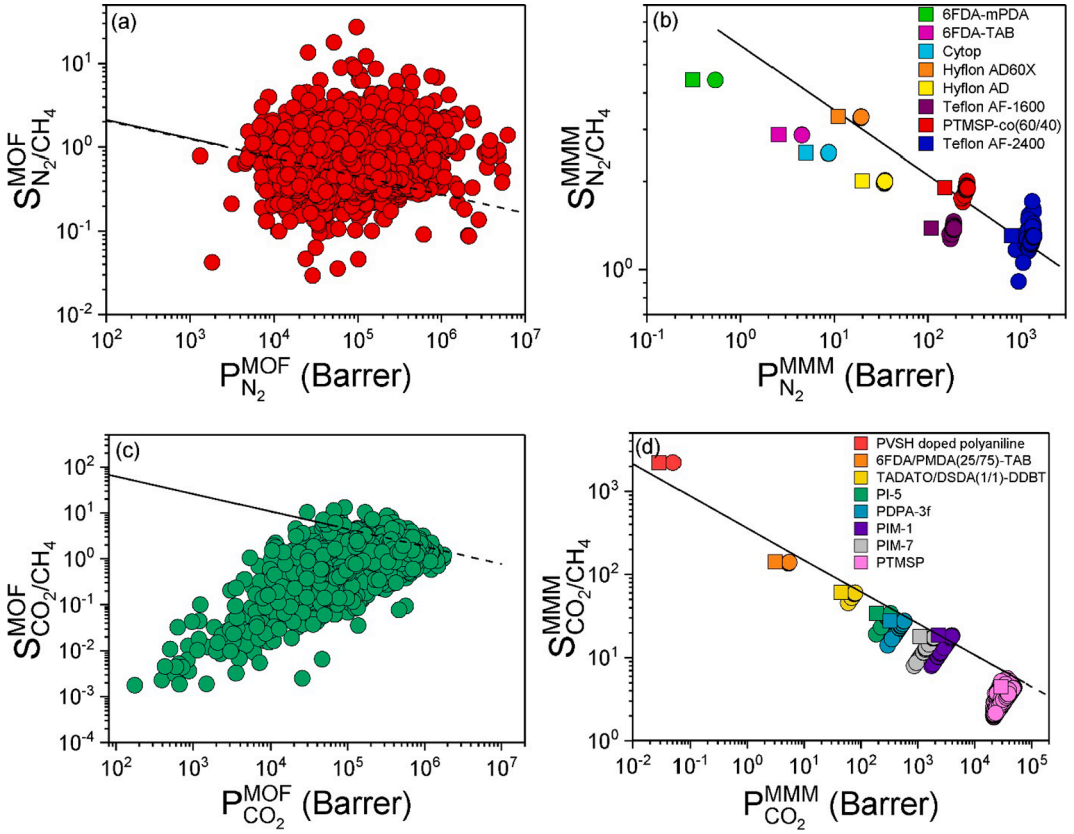


Fig. 2. N_2 permeabilities and N_2/CH_4 selectivities of (a) 5599 MOFs, (b) 44,792 MOF/polymer MMMs composed of 8 polymers and 5599 MOFs. CO_2 permeabilities and CO_2/CH_4 selectivities of (c) 2124 MOFs, (d) 16,992 MOF/polymer MMMs composed of 8 polymers and 2124 MOFs. Squares (circles) represent pure polymer (MOF/polymer MMM composed of the polymer shown with the same color) in (b) and (d). Black line is the Robeson's upper bound.

experimentally reported permeabilities of polymers. A significant number of MOFs (3701) was found to be above the Robeson's upper bound due to their high N_2 permeabilities and/or high N_2/CH_4 selectivities, indicating that these MOFs can be good fillers to improve the gas separation performances of polymers. We computed the separation performances of 44,792 MOF/polymer MMMs using 8 different polymers and 5599 MOFs.

Fig. 2(b) shows that all MOF fillers improve N_2 permeability of polymers having medium permeability <500 Barrer with slight or no change in N_2/CH_4 selectivity. On the other hand, N_2/CH_4 selectivities of highly permeable polymers (>1000 Barrer) increase, decrease, or do not change upon the incorporation of MOFs. Overall, these results showed that while MMMs composed of polymers having low permeability such as Cytop, 6FDA-mPDA, Hyflon AD, and Teflon AF-1600 remain under the upper bound, some MOFs carry the polymers, Hyflon AD60X, Teflon AF-2400 and PTMSP-co(60/40), well above the upper bound for N_2/CH_4 separation. Similar to the difficulty of separating N_2 from CH_4, membrane materials generally have low selectivity for air separation (O_2/N_2). As shown in Fig. S3(a), O_2 permeabilities and O_2/N_2 selectivities of 5599 MOFs were computed to be in a large range of 2.4×10^3–4×10^6 Barrers and 0.13–22.2, respectively. We estimated O_2 permeability and O_2/N_2 selectivity of 44,792 MOF/polymer MMMs as shown in Fig. S3(b) and concluded that BPDA-ODA, BADBSBF-BTDA, PIM-1, PIM-7, and PTMSPDA exceed the upper bound when MOFs are used as fillers. O_2/N_2 separation performances of MOF/polymer MMMs were discussed in detail by performing simulation at different conditions including infinite dilution, binary (O_2/N_2) and ternary (O_2/N_2/Ar) mixtures in our previous work [26].

CO_2 permeability and CO_2/CH_4 selectivity of MOFs were shown in Fig. 2(c). CO_2 permeabilities of 2124 MOFs were computed as 175–1.79×10^6 Barrers and CO_2/CH_4 selectivities were calculated to be between 1.76×10^{-3} and 13. Although 454 MOFs are CO_2 selective (S_{mem}^{MOF} >1.5), only 96 MOFs exceeded the upper bound. In Fig. 2(d), CO_2 permeability and CO_2/CH_4 selectivity of 16,992 MOF/polymer MMMs comprised of 2124 MOFs and 8 different polymers were shown. For MOF/polymer MMMs, we computed the maximum achievable CO_2 permeability as 4.95×10^4 Barrer and CO_2/CH_4 selectivity as 2200. MOF fillers increase CO_2 permeability of two polymers, PSVH doped polyaniline and 6FDA/PMDA(25/75)-TAB, without changing their selectivity. We note that since PSVH doped polyaniline is already above the upper bound, all MMMs including PSVH doped polyaniline also exceed the bound. One important feature of Fig. 2(d) is that PIM-1 is the only polymer that is below the upper bound but surpasses it when certain types of MOF fillers are incorporated. We observed the similar results for CO_2/N_2 separation. CO_2 permeability of 2124 MOFs alter from 175 to 1.79×10^6 Barrers and CO_2/N_2 selectivities are between 1.64×10^{-3} and 14 as shown in Fig. S4(a). Similar to CO_2/CH_4 separation, majority of MOFs does not surpass the upper bound due to the low CO_2 permeability, low CO_2/N_2 selectivity, or both. These low CO_2 permeability and selectivity values of MOFs can be explained by the simulation conditions. In the previous computational screening studies [45,55,56], molecular simulations were generally performed at infinite dilution condition (considering only one gas molecule in the framework). Since single-component gas permeabilities are generally measured for polymers, we performed molecular simulations considering single-component gases. CO_2 permeability and CO_2/N_2 selectivity of MOFs computed at infinite dilution are in a larger range (4.9×10^3–8.1×10^9 Barrers and 7.68×10^{-2}–6.2×10^3, respectively) [25] compared to those obtained in this work for single-component gases at 1 bar, 298 K. This agrees with the previous findings where adsorption selectivity of MOFs was generally computed to be high at infinite dilution [26,57,58]. In Fig. S4(b), CO_2 permeabilities and CO_2/N_2 selectivities of 10,620 MOF/polymer MMMs composed of 5 polymers and 2124 MOFs are shown. CO_2 permeabilities of polymers increase, decrease, or remain the same with the addition of MOF fillers while selectivities of polymers generally remain constant. The maximum achievable CO_2 permeability and CO_2/N_2 selectivity among the performances of 10,620 MOF/polymer MMMs were estimated as 4.95×10^4 Barrer and 62.5, respectively. Huang et al. [59] discussed that the membrane materials exhibiting CO_2 permeability >100 Barrer and CO_2/N_2 selectivity >50 are required for economic operations. Thus, there are many MMMs which may meet the economic standards for CO_2/N_2 separation.

In the membrane industry, H_2/CH_4, H_2/N_2, and H_2/CO_2 separations play a vital role to meet the increasing demand for high purity hydrogen [60]. We computed H_2 permeabilities and membrane selectivities of MOFs and MOF/polymer MMMs in Fig. 3. Fig. 3(a) illustrates that while H_2 permeabilities of MOFs vary from 4.14×10^3 to 2.35×10^6 Barrers, their H_2/CH_4 selectivities were computed in the range of 1.66×10^{-2} and 50. A significant number of MOFs (2539) was found to be above the upper bound due to their high selectivity, or high permeability, or both. Fast diffusion of H_2 through the highly porous MOFs leads to high permeability and MOFs with narrow pores can limit the diffusion of strongly adsorbed CH_4 resulting in very high diffusion and membrane selectivity for H_2 over CH_4. We calculated H_2 permeability and H_2/CH_4 selectivity of 19,530 MOF/polymer MMMs composed of 3255 MOFs and 6 different polymers as shown in Fig. 3(b). The maximum achievable H_2/CH_4 selectivity and H_2 permeability of a MMM was computed as 325 and 4×10^4 Barrer, respectively. Results in Fig. 3(b) can be discussed as follows: (i) If a polymer has low permeability (<100 Barrer), any MOF can improve the H_2 permeability of polymers without changing the H_2/CH_4 selectivity. For example, MOF/DAPHFDS(H) MMMs have higher H_2 permeabilities (86–91 Barrers) than the pure polymer (52 Barrer) and have similar H_2/CH_4 selectivities (319–325) compared to the pure polymer (325). (ii) For polymers that have medium H_2 permeability (<500 Barrer), all MMMs have higher H_2 permeability than that of the polymer and a small number of MOFs slightly alters the selectivity of the polymer. (iii) If a polymer is highly permeable (>1000 Barrer), separation performance of the MOF fillers becomes the determining factor, and incorporation of MOFs can increase, decrease, or sustain the permeability and selectivity of the polymer. To illustrate, when MOFs are used in pure PTMSP-co(95/5) (H_2 permeability of 2.04×10^4 Barrer and H_2/CH_4 selectivity of 0.95), MMMs were found have a large range of H_2 permeabilities (1.63×10^4–3.52×10^4 Barrers) and H_2/CH_4 selectivities (0.56–1.8). Thus, many MOFs carry the polymers (DAPHFDS(H), 6FDA-DDBT, Hyflon AD60X, Teflon AF-2400, PTMSP, and PTMSP-co (95/5)) above the upper bound for H_2/CH_4 separation.

H_2 permeability and H_2/N_2 selectivities of 3255 MOFs were found to vary in the range of 4.14×10^3–2.35×10^6 Barrers and 2.13×10^{-2}–54.6, respectively as shown in Fig. 3(c). Similar to H_2/CH_4 separation, over 60% of MOFs surpass the upper bound. Using these data for MOFs, we computed H_2 permeability and H_2/N_2 selectivity of 22,785 MOF/polymer MMMs including 7 polymers and 3255 MOFs. The maximum achievable H_2 permeability and H_2/N_2 selectivity were calculated as 3.9×10^4 Barrer and 960, respectively. A significant message from Fig. 3(d) is that when MOF fillers are used, many polymers, PBOI-2-Cu^+, NTDA-BAPHFDS(H), PAI-3a, PIM-7, PIM-1, PTMSP, and PTMSP-co(95/5), surpass the upper bound with the increase in their H_2 permeability and/or H_2/N_2 selectivity.

Fig. S5(a) shows that H_2 permeabilities and H_2/CO_2 selectivities of 1194 MOFs were in a broad range of 4.7×10^3–1.68×10^6 Barrers and 5.11×10^{-2}–338, respectively. In contrast to the trade-off of polymers, H_2 permeability and H_2/CO_2 selectivity of MOFs are positively correlated. Majority of MOFs (969 out of 1194) surpasses the upper bound, which shows their high potential for H_2/CO_2 separation. We computed H_2 permeability and H_2/CO_2 selectivity of 3582 MOF/polymer MMMs including 1194 MOFs and 3 different polymers as shown in Fig. S5(b). When MOF fillers were added, H_2 permeabilities of all polymers increased without any significant change in their H_2/CO_2 selectivities. This can be explained with the low permeability of polymers (<100 Barrer) that defined the upper bound for H_2/CO_2 separation. Overall, the enhancement in H_2 permeabilities of polymers brings all MMMs,

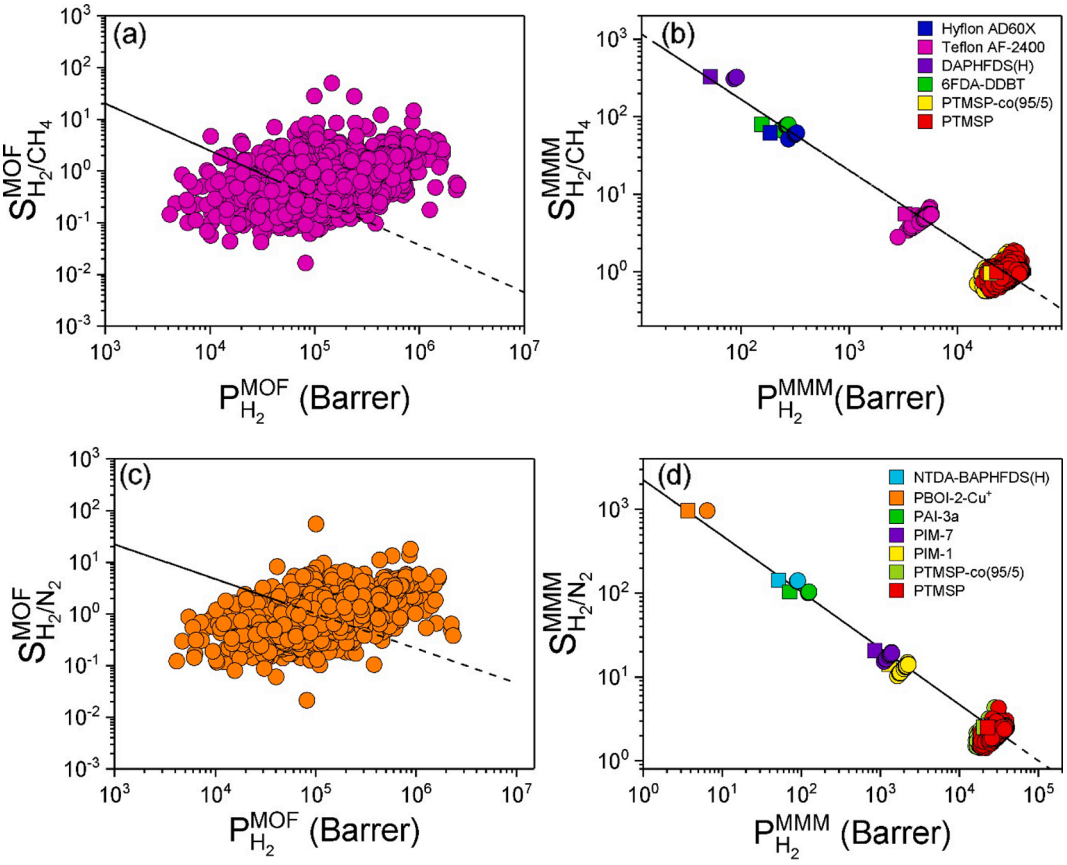


Fig. 3. H_2 permeabilities and H_2/CH_4 selectivities of (a) 3255 MOFs, (b) 19,530 MOF/polymer MMMs composed of 6 polymers and 3255 MOFs. H_2 permeabilities and H_2/N_2 selectivities of (c) 3255 MOFs, (d) 22,785 MOF/polymer MMMs composed of 7 polymers and 3255 MOFs. Squares (circles) represent pure polymer (MOF/polymer MMM composed of the polymer shown with the same color) in (b) and (d). The black line is the Robeson's upper bound.

including 1,1-6FDA-DIA with the increase in its H_2 permeability from 31 up to 55 Barrers, well above the upper bound. Recently, Ortiz et al. [61] tested the performances of three commercial H_2-selective membranes (PEI, PES, PBI) for H_2 purification applications (H_2/N_2, H_2/CH_4 and H_2/CO_2). They showed that although very high H_2 purities are obtained (>98%) with H_2 permeability (0.52–10.5 Barrers), H_2/N_2 selectivity (131–281), H_2/CH_4 selectivity (155–400) and H_2/CO_2 selectivity (1.9–3.7), these materials are still far from meeting the fuel cell quality standards. At this point, many MOF/polymer MMMs studied in this work deserve to be considered since they provide a wide range of H_2 permeability (0.1–2.2 × 10^4 Barrers), and H_2/N_2 (1.4–960), H_2/CH_4 (0.6–325) and H_2/CO_2 (8–101) selectivities.

We finally discussed the separation potential of MOFs and MOF/polymer MMMs for the purification of a noble gas, helium (He/H_2, He/N_2, He/CH_4, He/CO_2), since it has an essential role in various medical and industrial applications [62]. Fig. 4 represents 864 MOFs and 6048 different MOF/polymer MMMs for He/N_2 separation, 314 MOFs and 1884 MOF/polymer MMMs for He/CO_2 separation. To the best of our knowledge, such a large number of MOFs and MOF/polymer MMMs has not been investigated before for He-related separations in the literature. For He/N_2 separation, He permeabilities and He/N_2 selectivities of 864 MOFs were predicted in the range of 8.06 × 10^3–2.09 × 10^6 Barrers and 0.12–6.1, respectively, as shown in Fig. 4(a). Almost all MOFs (767 out of 864) surpass the upper bound, indicating that there is an opposite permeability/selectivity behavior compared to conventional polymeric membranes. When He permeabilities of MOFs increase, their He/N_2 selectivities also increase. After incorporation of MOF fillers into the polymers, He permeabilities and He/N_2 selectivities of MMMs were computed to be between 39.2 and 1.13 × 10^4 Barrers and 0.8–622, respectively. A conclusion from Fig. 4(b) is that all MOF fillers improve He permeability of almost all polymers except PTMSP with slight changes in membrane selectivities. For example, a MOF (refcode: GITTUZ) increases He permeability of the pure TMHFBPA-I/T from 182 to 307 Barrers whereas He/N_2 selectivity slightly decreases from 64.8 to 62.6. Fig. 4(b) also shows that if polymers are very close or already above the upper bound, using MOF fillers carries MMMs well above the upper bound. For example, all MOF/Hyflon AD MMMs exceed the upper bound by increases in the He permeability from 405 up to 658–709 Barrers.

We computed He permeability and He/CH_4 selectivity of MOFs in the range of 8.06 × 10^3–2.09 × 10^6 Barrers and 0.02–4.2, respectively, as shown in Fig. S6(a), showing that many MOFs outperform traditional polymers. The upper limits of He permeability and He/CH_4 selectivity of 3456 MMMs composed of 864 MOFs and 4 different polymers were computed as 6.28 × 10^3 Barrer and 3041, respectively, as shown in Fig. S6(b). These results indicate that many MOFs can improve the He permeability of polymers (6FDA/PMDA(10/90)-TAB, 6FDA-TAB, Hyflon AD60X and Teflon AF-2400) and carry MMMs well above the upper bound.

He permeabilities and He/CO_2 selectivities of MOFs vary from 8.06 × 10^3 to 2.09 × 10^6 Barrers and from 3.63 × 10^{-2} to 4.5, respectively, as shown in Fig. 4(c). 91% of MOFs exceed the upper bound and there is a linear correlation between selectivity and permeability of MOFs in contrast to the slope of the upper bound. He permeability and He/CO_2 selectivity for 1884 MOF/polymer MMMs membranes including 6 polymers and 314 MOFs were also computed as shown in Fig. 4(d). The highest values of permeability and selectivity were found as 6.37 × 10^3 Barrer and 20, respectively. For all polymers, addition of MOFs improved the permeabilities of polymers regardless of the identity of MOFs. In terms of selectivity, the performance of all polymers generally

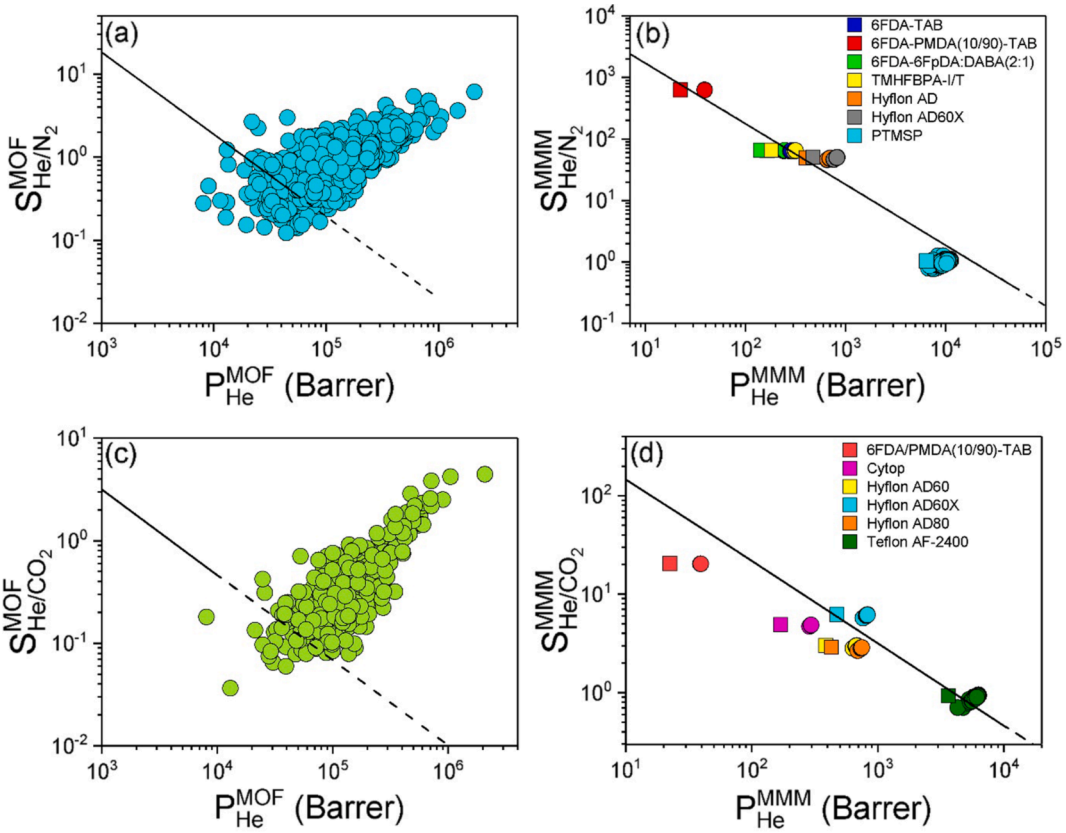


Fig. 4. He permeabilities and He/N_2 selectivities of (a) 864 MOFs, (b) 6048 MOF/polymer MMMs composed of 7 polymers and 864 MOFs. He permeabilities and He/CO_2 selectivities of (c) 314 MOF membranes (d) 1884 MOF/polymer MMMs composed of 6 polymers and 314 MOFs. Squares (circles) represent pure polymers (MOF/polymer MMMs composed of the polymer shown with the same color) in (b) and (d). Black line is the Robeson's upper bound.

remained the same with the incorporation of MOFs. As a result, all MMMs with Hyflon AD60X and some of the MMMs composed of Teflon AF-2400 surpass the upper bound for He/CO_2 separation.

Fig. S7(a) shows that while He permeabilities of MOFs were computed to be in a broad range (8.06×10^3–2.09×10^6 Barrers), He/H_2 membrane selectivities were close to 1, in a narrow range (0.1–2.4) due to the similar adsorption and diffusion properties of He and H_2 in MOFs. Almost 21% of MOFs outperform the polymers which establish the upper bound. Fig. S7(b) shows that upper limits of He permeabilities and He/H_2 selectivities of 6768 MOF/polymer MMMs were calculated as 6.28×10^3 Barrer and 4.4, respectively. If the gas permeability of a MOF is significantly higher than that of a polymer, the maximum achievable gas permeability of the MMM calculated by Maxwell model is equal to 1.75 times the permeability of the polymer [21,24,26]. For example, MOF fillers increase the He permeability of the Hyflon AD60X (476 Barrer) up to 75% and He permeabilities of all MOF/Hyflon AD60X MMMs were found to be in the range of 765–833 Barrers in Fig. S7. Overall, we showed that while the MMMs of many polymers are below the upper bound, two polymers (Nafion 117 and Hyflon AD60X) are the best choices to comprise high performing MMMs with MOFs as they are closer to the upper bound compared to other polymers. To the best of our knowledge, PSA and cryogenic distillation methods currently dominate the helium recovery from natural gas and there is no large-scale membrane used for helium purification [63]. Since cellulose acetate membranes are currently used in membrane industry, they have been considered as potential candidates to be used in helium purification applications (He/N_2, He/CH_4, He/CO_2, He/H_2) [62]. If the separation potentials of MOF/polymer MMMs that we determined for He/N_2 separation (He permeability: $39.2–1.13 \times 10^4$ Barrers, He/N_2 selectivity: 0.8–622) are compared with those of cellulose acetate membranes (He permeability: 13.6 Barrer, He/N_2 selectivity: 48.6), there are several MOF/polymer MMMs which provide a separation performance well beyond the desired performances, emphasizing the huge potential of the incorporation of MOFs as fillers into polymers.

To better understand the potential of MMMs we examined in this work, their gas permeability and selectivity are compared with those of experimentally reported MMMs. We collected experimentally available data of 49 different MOF/polymer MMMs from various works in the literature. Experimental measurement conditions such as temperature, pressure, and volume fraction of MOFs in MMMs are provided in Table S14. Fig. S8 shows that separation performances of commonly synthesized MMMs were generally below the upper bound. Many MOF/polymer MMMs that we considered in this work have not been experimentally or computationally studied before and our results showed that many of them can be well above the upper bound for various gas separations, indicating their promise. For example, Fig. S8 shows that MMMs synthesized by using common polymers such as PIM-1, Matrimid and MOFs such as ZIF-8, Cu-BTC do not have high enough permeability and selectivity to surpass the upper bound for He-based separations. On the other hand, our results showed that if polymers such as Hyflon AD60X and Teflon AF-2400 are used to make MOF/polymer MMMs, they can exceed the upper bound due to their high He permeability and/or selectivity. Although the number of synthesized MMMs for which we collected the data from literature is low compared to the number of MMMs that we studied using molecular simulations, this comparison is still useful to highlight the potential of MOF/polymer MMMs that have not been synthesized yet. Our results also reveal the importance of studying the entire MOF database and large number/variety of polymers rather than focusing on a small number/type of MOFs and polymers.

We also compared the performance of MOF and MOF-based MMMs with those of zeolites. Several zeolites are already above the Robeson's upper bound for different gas separations. For instance, chabazite

zeolites such as SAPO-34 display remarkable separation performance for CO_2/CH_4 [64] and He/CH_4 [65] and exceed the upper bound. Krishna and van Baten [66] showed that CHA, DDR and FAU surpass the upper bound for CO_2/N_2 separation. Some of the zeolite membranes show higher performances compared to MOF-based MMMs. For example, DDR zeolite has a similar CO_2 permeability compared to simulated MOF/PTMSP MMMs which have the highest CO_2 permeability (4.95×10^4 Barrer). However, selectivity of DDR (19) is almost twofold compared to the highest selectivity of MOF/PTMSP MMMs (11) for CO_2/N_2 separation. In the same CO_2 permeability range, ERI zeolite shows similar selectivity values (12) to our results for MOF/PTMSP MMMs. On the other hand, TSC zeolite displays a lower performance compared to our results and it is located below the Robeson's upper bound. Overall, separation performances of MOF/polymer MMMs that we studied are comparable to several zeolite membranes.

3.3. Assessment of MOF-polymer pairing

Our aim in this work is to present guidelines for the selection of the best MOF-polymer combinations depending on the type of the gas separation. We showed in Figs. 2-4 and Figs. S3-S7 that while some polymers were tested only for a single type of gas separation, many polymers were used to separate different gas pairs. To identify the best combination of MOF-polymer pairs for MMM applications, understanding how the polymer selection affects the performances of MMMs for different gas separations is important. In this work, we computed permeabilities for a large variety of gases and for the largest number of MOF/polymer MMMs reported in the literature: He permeability of 12,960 MMMs including 864 MOFs and 15 polymers, CO_2 permeability of 40,356 MMMs including 2124 MOFs and 19 polymers, O_2 permeability of 44,792 MMMs including 5599 MOFs and 8 polymers, H_2 permeability of 65,100 MMMs including 3255 MOFs and 20 polymers, CH_4 permeability of 111,980 MMMs including 5599 MOFs and 20 polymers, and N_2 permeability of 145,574 MMMs including 5599 MOFs and 26 polymers were studied. Studying large number of MMMs for a variety of gases enabled us to offer a guideline for identifying the best MOF-polymer pairs for each separation.

Fig. 5 visualizes how the gas permeability and selectivity of polymers change when MOF fillers are incorporated to generate a MOF/polymer MMM for different gas separations. The number of MOFs and polymers used in MMMs for each gas separation can be seen in Fig. 5(a). Each cell in Fig. 5(b) and (c) demonstrates the effect of MOF filler on the gas separation performances of polymers. Red, yellow, and blue regions represent MOF/polymer MMMs offering higher, similar, and lower gas permeability than those of the corresponding pure polymers, respectively in Fig. 5(b). Similar representation for selectivity is given in Fig. 5(c). We note that if a MOF does not affect the gas permeability or selectivity of a polymer in the range of ±10%, we include this MOF filler in the yellow region in Fig. 5(b) and (c).

Fig. 5(b) clearly shows that addition of MOF fillers into the polymers increases the permeability of all gases in almost all polymers, represented with red regions. The improvements in gas permeability of MOF/polymer MMMs can be explained by the high permeabilities of MOFs due to their highly porous structures. In the membrane industry, achieving high gas permeability is strongly desired because highly permeable membranes require low surface area and low capital cost [67]. Thus, Fig. 5(b) highlights the potential of using MOF/polymer MMMs for a large variety of gas separations. We also note that there are some minor cases for which some MOF fillers decrease or do not alter the gas permeability of polymers (e.g., PTMSP-co(95/5) for N_2 and CH_4, PTMSP for CO_2 and CH_4, PTMGP for CO_2).

The impact of MOF filler on the membrane selectivity of polymers is shown in Fig. 5(c). Using MOF fillers generally keeps the membrane selectivities of polymers the same, represented with large yellow regions. This result can still be considered as promising because many MOF/polymer MMMs can exceed the upper bound with the enhancement only in gas permeability for most gas separations as we discussed before. MOF fillers can have a negative impact on the membrane selectivity of some polymers although the decrease in membrane selectivity is generally small. For example, H_2/N_2 selectivity of PTMSP decreased from 2.5 to 1.4 after incorporation of some MOFs. As a result, using a small number of MOF fillers leads to a slight decrease in the membrane selectivity of polymers such as PIM-7, PIM-1, PTMSP, MEEP, PTMGP for CO_2/N_2, 6FDA-DDBT, Hyflon AD60X, PTMSP-co(95/5), Teflon AF-2400, PTMSP for H_2/CH_4, PTMSP for He/N_2, PIM-7, PIM-1, PTMSP-co(95/5), PTMSP for H_2/N_2, Teflon AF-2400 for N_2/CH_4, He/CH_4, He/CO_2 and He/H_2, PIM-7, PIM-1, PTMSP, PI-5, PDPA-3f for CO_2/CH_4, PTMSPDPA and PIM-1 for O_2/N_2 separation.

Results showed that small number MOF fillers also improve the membrane selectivity of polymers such as Teflon AF-2400 for H_2/CH_4, N_2/CH_4, PTMSP-co(95/5) for H_2/CH_4, H_2/N_2, PTMSP for H_2/CH_4, He/N_2, H_2/N_2, CO_2/CH_4, and PTMSDPA for O_2/N_2 separation. We finally note that a MOF filler can differently affect the membrane selectivity of a polymer for different gas separations. For example, incorporation of a MOF doubles the H_2/N_2 selectivity of PTMSP-co(95/5) from 2.5 to 4.3, while the same MOF does not change selectivity of the same polymer (from 0.95 to 1.1) for H_2/CH_4 separation. Overall, among these 41 polymers, Fig. 5 indicates that 4 polymers, PTMSDPA, Teflon AF-2400, PTMSP-co(95/5), and PTMSP have a great potential for improved gas permeability and selectivity when used in MOF/polymer MMM applications.

3.4. Structure-performance relations

In this section, structural properties of MOF and the separation performances of MMMs were studied by focusing on N_2/CH_4 and H_2/N_2 since the largest number of MMMs (44,792, and 22,785, respectively) were examined for these gas pairs. We selected the highly permeable polymers, Teflon AF-2400 for N_2/CH_4 and PTMSP for H_2/N_2 separations. Fig. 6 shows the porosity and PLD of MOF fillers and is color-coded based on the selectivities of MMMs. As expected, MOFs with large PLDs generally have high porosities and vice versa. Similar to the color-coding in Fig. 5(c), red, yellow, and blue symbols represent the MOFs that improve, do not change, and impair the selectivity of related polymer, respectively. We note that all MOF sets that are used for N_2/CH_4 and H_2/N_2 separations are representative in terms of PLDs (3.7–71 Å) and porosities (0.26–0.94).

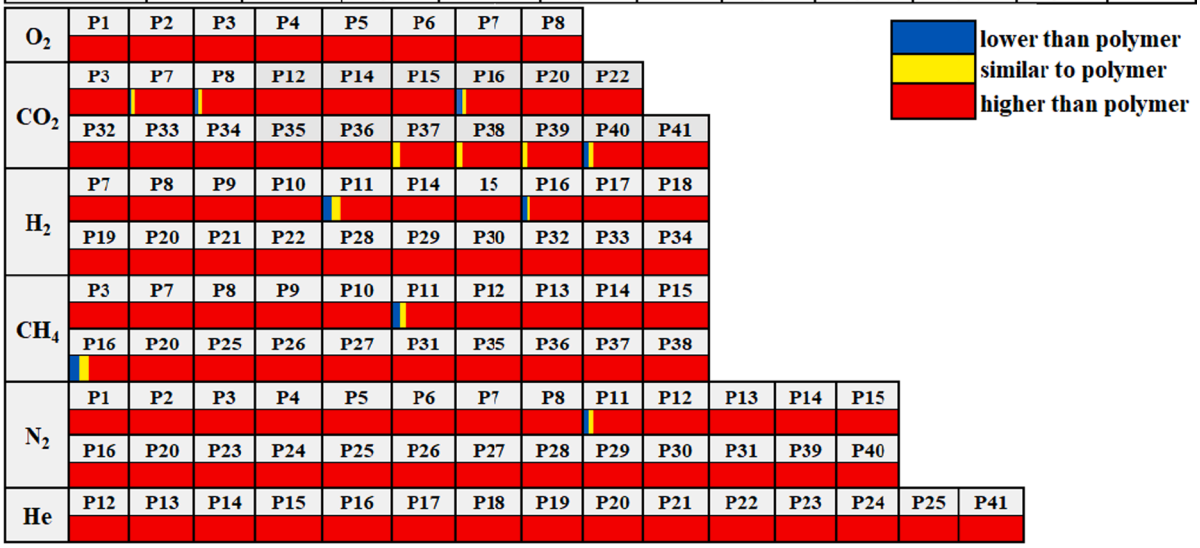
Fig. 6(a) shows that the best MOF fillers that improve the selectivity of Teflon AF-2400 for N_2/CH_4 separation exhibit very narrow PLDs (3.7–4.1 Å) and low porosities (0.35–0.51). These MOFs also have a narrow LCD range (4.3–5.3 Å) and low S_{acc} (<1060 m^2/g). For H_2 related gas separations, Fig. 6(b) shows that MOF/PTMSP MMMs exhibiting significantly higher H_2/N_2 selectivity (2.8–4.3) than the pure PTMSP (2.5) are obtained with MOFs having a larger range of PLDs (3.8–11.2 Å) and porosities (0.41–0.73) than those observed for N_2/CH_4 separation. In addition, these MOFs have a larger range of LCD (4.7–18.4 Å) and S_{acc} (161–2682 m^2/g). We note that a MOF filler can improve the selectivity of a polymer in one of the gas separations whereas the same filler can have negative or no impact on the selectivity in another gas separation. For example, while a MOF filler (refcode: TONWUO) decreases the H_2/N_2 membrane selectivity of PTSMP from 2.5 to 2.2, the same MOF increases the N_2/CH_4 membrane selectivity of Teflon AF-2400 from 1.3 to 1.6. One of the important messages of Fig. 6 is that none of the MOFs having large pore sizes (>20 Å) and high porosities (>0.85) affect the selectivity of PTMSP and Teflon AF-2400 for these two gas separations. As a result, we concluded that the MOFs with narrow pores (<10 Å), small porosities (<0.6) and low surface area (<1060 m^2/g) become the top fillers which improve the membrane selectivity of polymers in N_2/CH_4 and H_2/N_2 separations.

We finally provided a detailed discussion of the assumptions that we used in our computational approach since these assumptions may affect our predictions for the gas separation performances of MOF-based

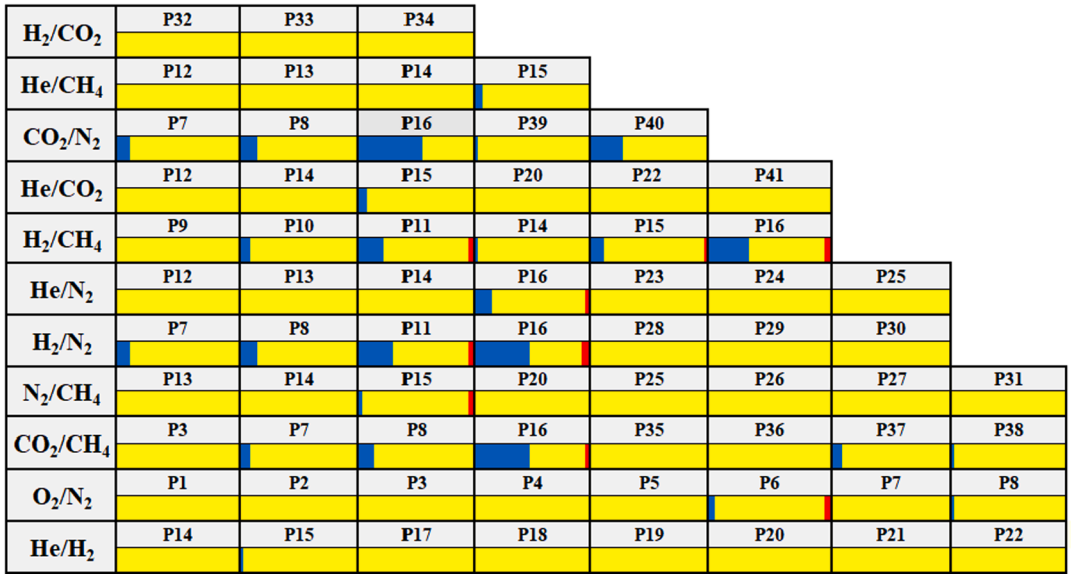
(a)

	H_2/CO_2	He/CH_4	CO_2/N_2	He/CO_2	H_2/CH_4	He/N_2	H_2/N_2	N_2/CH_4	CO_2/CH_4	O_2/N_2	He/H_2
# of MOF	1194	864	2124	314	3255	864	3255	5599	2124	5599	846
# of Polymer	3	4	5	6	6	7	7	8	8	8	8
# of MMM	3582	3456	10,620	1884	19,530	6048	22,785	44,792	16,992	44,792	6768

(b)



(c)



P1: BPDA-ODA	**P12**: 6FDA-PMDA(10/90)-TAB	**P23:** 6FDA-6FpDA:DABA(2:1)	**P34:** 1,1-6FDA-DIA
P2: Polyetherimide	**P13**: 6FDA-TAB	**P24:** TMHFBPA-I/T	**P35:** PVSH doped polyaniline
P3: 6FDA/PMDA(25/75)-TAB	**P14**: Hyflon AD60X	**P25:** Hyflon AD	**P36:** TADATO/DSDA(1/1)-DDBT
P4: Sulfonated brominated PPO	**P15**: Teflon AF-2400	**P26:** 6FDA-mPDA	**P37:** PI-5
P5: BADBSBF-BTDA	**P16**: PTMSP	**P27:** PTMSP-co(60/40)	**P38:** PDPA-3f
P6: PTMSDPA	**P17**: Viton E60	**P28**: PBOI-2-Cu $^{+}$	**P39:** MEEP
P7: PIM-7	**P18:** Nafion 117	**P29**: NTDA-BAPHFDS(H)	**P40:** PTMGP
P8: PIM-1	**P19:** Viton GF	**P30**: PAI-3a	**P41:** Hyflon AD60
P9: DAPHFDS(H)	**P20:** Cytop	**P31**: Teflon AF-1600	
P10: 6FDA-DDBT	**P21:** Fluorinated Polynorbornene	**P32:** Liquid polyester (HBA/HNA-30/70)	
P11: PTMSP-co(95/5)	**P22:** Hyflon AD80	**P33:** Polyaniline (redoped)	

Fig. 5. (a) The number of studied MOFs, polymers and MOF/polymer MMMs. The impact of MOFs on (b) gas permeabilities and (c) selectivities of polymers. Red and blue indicate that MMMs exhibit higher and lower values compared to the pure polymer. Yellow represents that MMMs have similar performances (±10%) to those of the corresponding polymer. (For interpretation of the references to color in this figure legend, the reader is referred to the web version of this article.)

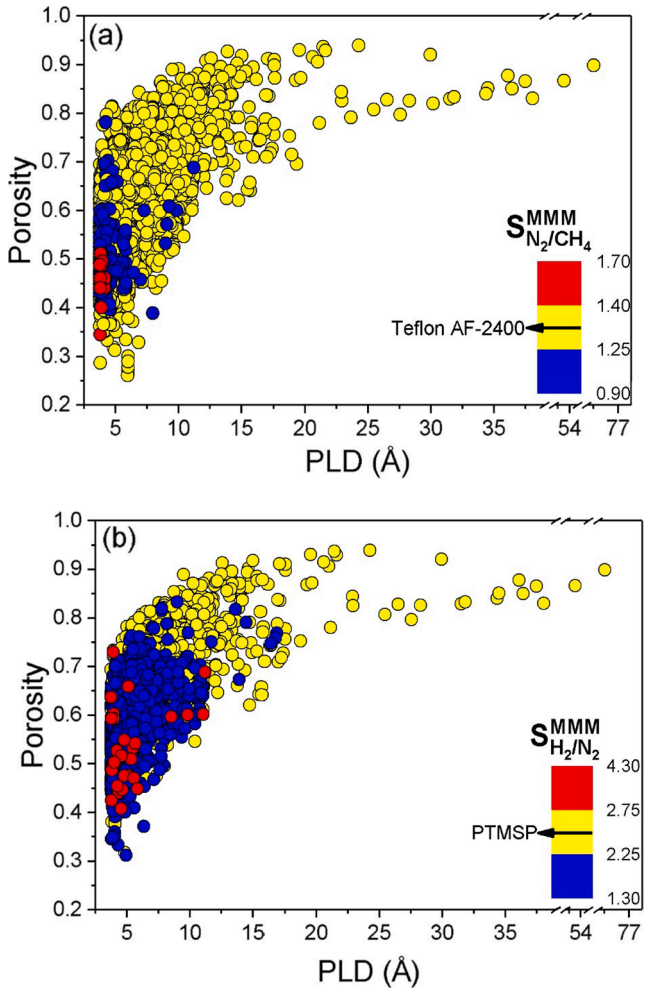


Fig. 6. The relationship between structural properties of MOFs and selectivities of MMMs for (a) N_2/CH_4, (b) H_2/N_2 separations.

MMMs. We computed the membrane properties of MOFs by using rigid frameworks in molecular simulations. Flexible simulations of MOFs require significant computational time and developing an accurate force field for flexible MOFs to consider the bonded terms of framework atoms is not straightforward. Rigid framework assumption is a good approximation to compute the adsorption properties except for the MOFs exhibiting structural phase transition upon gas adsorption [68,69]. However, structural flexibility may influence the gas diffusion properties of MOFs. Sholl and coworkers extensively compared the computed diffusion coefficients from both rigid and flexible simulations for noble gas [70], small alcohols [71], CO_2 and CH_4 [72]. They showed that using a rigid framework generally led to lower diffusivities compared to those obtained with using a flexible structure since rigid frameworks can prevent the diffusion of gas molecules. Haldoupis et al. [73] showed that CH_4 diffusion is too slow in rigid ZIF-8 due to the narrow pore sizes of ZIF-8 compared to the size of CH_4 molecules (~3.8 Å). We previously showed that structural flexibility has a significant effect on the gas permeability and membrane selectivity of MOFs having narrow pores close to the size of gas molecules for CO_2/CH_4 [21,74] and CH_4/H_2 [75] separation.

In this work, since we considered only the MOFs with pore sizes larger than the sizes of the six gas molecules, we expect that structural flexibility of MOFs will have a negligible effect on the overall results. It is not possible to study >180,000 materials by considering flexibility for all of them due to the computational expense of flexible simulations. To examine the effect of structural flexibility of MOFs on the predicted separation performances of MOF/polymer MMMs, we focused on O_2/N_2 separation, which is the gas pair including one of the largest molecules in this work. Two MOFs were selected by considering the ranking of MOF/PTMSDPA MMMs based on their selectivities. These two MOFs are the representatives of narrow-pored (refcode: TUBJAD, PLD: 4.4 Å) and large-pored (refcode: XADCEM, PLD: 8.1 Å) materials for the systematic investigation of the effect of flexibility. We performed flexible MD simulations using the loadings obtained at 1 bar, 298 K. More details of these flexible simulations were provided in our previous study [26]. We then used the Maxwell model to compute the single gas permeabilities and selectivities of 16 MOF/polymer MMMs composed of 2 MOFs and 8 different polymers. Fig. S9 compares the gas separation performances of MOFs and MOF/polymer MMMs obtained from rigid and flexible simulations. When flexibility was considered in the simulations of the MOF having large pores (XADCEM), O_2 permeability slightly decreased without changing O_2/N_2 selectivity as shown in Fig. S9(a). O_2 permeabilities and O_2/N_2 membrane selectivities of the MMMs have not been affected by the structural flexibility of the large-pored MOFs. On the other hand, Fig. S9(b) shows that when we considered the structural flexibility of the narrow-pored MOF (TUBJAD), both O_2 permeabilities and O_2/N_2 selectivities obtained from flexible simulations were considerably lower than those obtained from rigid simulations, moving the MOF below the upper bound but only slightly affecting O_2 permeabilities and O_2/N_2 membrane selectivities of the MOF/polymer MMMs. This result is in agreement with our previous report showing that although flexibility has a pronounced effect on the properties of the narrow-pored MOF membrane compared to that of the large-pored MOF membrane, the effect of flexibility on the predicted O_2 permeabilities and O_2/N_2 selectivities of the MMMs is negligible [26].

We finally note that even if the MMMs that we identified as the best are synthesized and tested, their performances may be expected to be lower than our predictions since we assumed perfect compatibility between the MOF and the polymer. For example, we previously showed that although predicted CO_2 and CH_4 permeabilities using the Maxwell model agree well with the experimental data at low filler loadings, predictions generally overestimated the experimental values as filler loading increased [50]. This can be explained with the inevitable defects observed in experimentally fabricated MMMs or agglomeration of MOF particles in the polymer which probably act as a non-selective region at the MOF-polymer interface. This is also supported by a recent computational study where fully atomistic simulations were performed to examine the effect of the interface between the MOF and polymer on the H_2/CH_4 separation performances of MMMs [76]. They showed that due to the non-selective voids at the interface of ZIF-8/PIM-1 MMMs, H_2/CH_4 selectivities of MMMs obtained from fully atomistic simulations were lower than the ones obtained by using a theoretical permeation model. In this study, since we aimed to explore the maximum achievable gas separation performances of MMMs, we did not consider the morphologic problems such as agglomeration of fillers, poor compatibility of filler and the polymer which may cause a negative effect on the separation performances of MMMs. Therefore, our calculations are based on a theoretical model (Maxwell) that considers the ideal morphology of MMMs. In addition to this, since morphological problems are more possible for increased filler loading, we fixed the filler volume fraction as 0.2 at which Maxwell model is noted to be applicable [77].

4. Conclusions

In this work, we identified the upper performance limits of MOF/polymer MMMs for various gas separation applications including helium, hydrogen, natural gas, and air purification. Gas permeability and selectivity of a total of 181,249 different MOF/polymer MMMs were examined using 5599 MOFs as fillers in 41 different polymers for 11 different separations, He/H_2, He/N_2, He/CH_4, He/CO_2, H_2/N_2, H_2/CH_4, O_2/N_2, CO_2/N_2, CO_2/CH_4, N_2/CH_4, H_2/CO_2. We highlight that this is the largest number of MOF/polymer MMMs in which synthesized, real

MOFs were considered as fillers using the results of high-throughput molecular simulations. With this study, potentials of MOF/polymer MMMs were revealed for all different gas separations for which Robeson's upper bound was defined. Our results showed that many polymers exceed the Robeson's upper bound due to the increase in their gas permeabilities and/or membrane selectivities upon MOF incorporation. Incorporation of MOF fillers increases the gas permeability of all polymers (41) that we considered in this study; therefore, the need of high membrane surface area and capital cost can decrease considerably. We compared the separation performances of the MOF/polymer MMMs that we considered in this work with the experimentally synthesized ones. Results showed that there are many promising MMMs which have not been experimentally tested yet for the related gas separations. A guide that visualizes how MOF fillers change the gas permeability and selectivity of polymers was generated and results showed that almost all MOFs that we studied improve He, H_2, N_2, CH_4, O_2 and CO_2 permeabilities of 41 different polymers while keeping their membrane selectivity constant. Results also revealed that if some polymers were specifically selected such as PTMSDPA for O_2/N_2 separation, PTMSP-co (95/5) for H_2/CH_4 and H_2/N_2 separations, Teflon AF-2400 for H_2/CH_4 and N_2/CH_4 separations, PTMSP for CO_2/CH_4, H_2/CH_4, He/N_2, H_2/N_2 separations, then MOF fillers improve not only the gas permeability but also the membrane selectivity of these polymers. Finally, structure-performance analysis showed that MOFs with PLDs <10 Å, porosities <0.6, and surface area <1060 m^2/g have potentials to increase the N_2/CH_4 and H_2/N_2 selectivity of the highly permeable polymers. We believe that the guidelines that we offer to aid the selection of promising MOF-polymer pairs will accelerate the experimental efforts for the synthesis of new MOF/polymer MMMs for target gas separations.

CRediT authorship contribution statement

Hilal Daglar: Investigation, Methodology, Validation, Software, Writing – original draft, Writing – review & editing. **Sena Aydin:** Investigation, Methodology, Validation, Software, Writing – original draft, Writing – review & editing. **Seda Keskin:** Conceptualization, Supervision, Methodology, Writing – review & editing.

Declaration of Competing Interest

The authors declare that they have no known competing financial interests or personal relationships that could have appeared to influence the work reported in this paper.

Acknowledgement

S.K. acknowledges ERC-2017-Starting Grant. This research has received funding from the European Research Council (ERC) under the European Union's Horizon 2020 research and innovation programme (ERC-2017-Starting Grant, grant agreement no. 756489-COSMOS).

Supporting Information (SI)

Computational workflow; comparison of experimental and simulated gas permeability of MOFs; potential parameters used in molecular simulations; experimentally reported permeabilities and selectivities of polymers for 11 different gas separations; measurement conditions of experimentally reported MOF/polymer MMMs; adsorption and diffusion properties of CO_2 and N_2 in MOFs; simulated gas permeability and selectivity of MOF/polymer MMMs for O_2/N_2, CO_2/N_2, H_2/CO_2, He/CH_4, and He/H_2 separations; experimentally measured gas separation performances of MOF/polymer MMMs; comparison of rigid and flexible simulation results for MOFs and MOF/polymer MMMs.

Appendix A. Supplementary material

Supplementary data to this article can be found online at https://doi.org/10.1016/j.seppur.2021.119811.

References

[1] O.R.N. Laboratory, Materials for Separation Technologies: Energy and Emission Reduction Opportunities, in, Oak Ridge National Laboratory Oak Ridge, 2005.
[2] Y. Ding, Perspective on gas separation membrane materials from process economics point of view, Ind. Eng. Chem. Res. 59 (2019) 556–568, https://doi.org/10.1021/acs.iecr.9b05975.
[3] W.J. Koros, G. Fleming, Membrane-based gas separation, J. Membr. Sci. 83 (1993) 1–80, https://doi.org/10.1016/0376-7388(93)80013-N.
[4] L.M. Robeson, The upper bound revisited, J. Membr. Sci. 320 (2008) 390–400, https://doi.org/10.1016/j.memsci.2008.04.030.
[5] L.M. Robeson, Correlation of separation factor versus permeability for polymeric membranes, J. Membr. Sci. 62 (1991) 165–185, https://doi.org/10.1016/0376-7388(91)80060-J.
[6] G. Deng, J. Luo, X. Liu, S. Liu, Y. Wang, X. Zong, S. Xue, Fabrication of high-performance mixed-matrix membranes via constructing an in-situ crosslinked polymer matrix for gas separations, Sep. Purif. Technol. 271 (2021), 118859, https://doi.org/10.1016/j.seppur.2021.118859.
[7] B. Zhang, Q. Yan, G. Chen, C. Yi, S. Qi, B. Yang, Fabrication of mixed matrix membranes with zinc ion loaded titanium dioxide for improved CO_2 separation, Sep. Purif. Technol. 254 (2021), 117472, https://doi.org/10.1016/j.seppur.2020.117472.
[8] K. Nocoń-Szmajda, A. Wolińska-Grabczyk, A. Jankowski, U. Szeluga, M. Wójtowicz, J. Konieczkowska, A. Hercog, Gas transport properties of mixed matrix membranes based on thermally rearranged poly(hydroxyimide)s filled with inorganic porous particles, Sep. Purif. Technol. 242 (2020), 116778, https://doi.org/10.1016/j.seppur.2020.116778.
[9] M. Rezakazemi, K. Shahidi, T. Mohammadi, Hydrogen separation and purification using crosslinkable PDMS/zeolite a nanoparticles mixed matrix membranes, Int. J. Hydrog. Energy 37 (2012) 14576–14589, https://doi.org/10.1016/j.ijhydene.2012.06.104.
[10] B. Zornoza, C. Téllez, J. Coronas, O. Esekhile, W.J. Koros, Mixed matrix membranes based on 6FDA polyimide with silica and zeolite microsphere dispersed phases, AIChE J. 61 (2015) 4481–4490, https://doi.org/10.1002/aic.15011.
[11] C.V. Funk, D.R. Lloyd, Zeolite-filled microporous mixed matrix (ZeoTIPS) membranes: Prediction of gas separation performance, J. Membr. Sci. 313 (2008) 224–231, https://doi.org/10.1016/j.memsci.2008.01.002.
[12] H. Furukawa, K.E. Cordova, M. O'Keeffe, O.M. Yaghi, The chemistry and applications of metal-organic frameworks, Science 341 (2013), https://doi.org/10.1126/science.1230444.
[13] R. Adams, C. Carson, J. Ward, R. Tannenbaum, W. Koros, Metal organic framework mixed matrix membranes for gas separations, Micropor. Mesopor. Mat. 131 (2010) 13–20, https://doi.org/10.1016/j.micromeso.2009.11.035.
[14] Q. Song, S. Nataraj, M.V. Roussenova, J.C. Tan, D.J. Hughes, W. Li, P. Bourgoin, M. A. Alam, A.K. Cheetham, S.A. Al-Muhtaseb, Zeolitic imidazolate framework (ZIF-8) based polymer nanocomposite membranes for gas separation, Energy Environ. Sci. 5 (2012) 8359–8369, https://doi.org/10.1039/C2EE21996D.
[15] Q. Qian, P.A. Asinger, M.J. Lee, G. Han, K. Mizrahi Rodriguez, S. Lin, F.M. Benedetti, A.X. Wu, W.S. Chi,f Z.P. Smith, MOF-based membranes for gas separations, Chem. Rev., 120 (2020) 8161-8266, 10.1021/acs.chemrev.0c00119.
[16] B. Seoane, V. Sebastián, C. Téllez, J. Coronas, Crystallization in THF: the possibility of one-pot synthesis of mixed matrix membranes containing MOF MIL-68 (Al), CrystEngComm 15 (2013) 9483–9490, https://doi.org/10.1039/C3CE40847G.
[17] K. Chen, K. Xu, L. Xiang, X. Dong, Y. Han, C. Wang, L.-B. Sun, Y. Pan, Enhanced CO_2/CH_4 separation performance of mixed-matrix membranes through dispersion of sorption-selective MOF nanocrystals, J. Membr. Sci. 563 (2018) 360–370, https://doi.org/10.1002/advs.201800982.
[18] E. Aliyev, J. Warfsmann, B. Tokay, S. Shishatskiy, Y.-J. Lee, J. Lillepaerg, N. R. Champness, V. Filiz, Gas Transport Properties of the Metal-Organic Framework (MOF)-Assisted Polymer of Intrinsic Microporosity (PIM-1) Thin-Film Composite Membranes, ACS Sustain. Chem. Eng. 9 (2020) 684–694, https://doi.org/10.1021/acssuschemeng.0c06297.
[19] A. Akbari, J. Karimi-Sabet, S.M. Ghoreishi, Matrimid® 5218 based mixed matrix membranes containing metal organic frameworks (MOFs) for helium separation, Chem. Eng. Process. 148 (2020), 107804, https://doi.org/10.1016/j.cep.2020.107804.
[20] F.H. Allen, The Cambridge Structural Database: A quarter of a million crystal structures and rising, Acta Crystallogr. Sect. B: Struct. Sci. 58 (2002) 380–388, https://doi.org/10.1107/S0108768102003890.
[21] C. Altintas, S. Keskin, Molecular simulations of mof membranes and performance predictions of mof/polymer mixed matrix membranes for CO_2/CH_4 separations, ACS Sustain. Chem. Eng. 7 (2019) 2739–2750, https://doi.org/10.1021/acssuschemeng.8b05832.
[22] T. Yan, Y. Lan, M. Tong, C. Zhong, Screening and design of covalent organic framework membranes for CO_2/CH_4 separation, ACS Sustain. Chem. Eng. 7 (2018) 1220–1227, https://doi.org/10.1021/acssuschemeng.8b04858.
[23] A.N.V. Azar, S. Velioglu, S. Keskin, Large-scale computational screening of metal organic framework (MOF) membranes and mof-based polymer membranes for $H_2/$

N_2 separations, ACS Sustain. Chem. Eng. 7 (2019) 9525–9536, https://doi.org/10.1021/acssuschemeng.9b01020.
[24] S. Budhathoki, O. Ajayi, J.A. Steckel, C.E. Wilmer, High-throughput computational prediction of the cost of carbon capture using mixed matrix membranes, Energy Environ. Sci. 12 (2019) 1255–1264, https://doi.org/10.1039/C8EE02582G.
[25] H. Daglar, S. Keskin, High-throughput screening of metal organic frameworks as fillers in mixed matrix membranes for flue gas separation, Adv. Theory Simul. 2 (2019) 1900109, https://doi.org/10.1002/adts.201900109.
[26] H. Daglar, I. Erucar, S. Keskin, Exploring the performance limits of MOF/polymer MMMs for O_2/N_2 separation using computational screening, J. Membr. Sci. 618 (2020), 118555, https://doi.org/10.1016/j.memsci.2020.118555.
[27] Y.G. Chung, E. Haldoupis, B.J. Bucior, M. Haranczyk, S. Lee, H. Zhang, K. D. Vogiatzis, M. Milisavljevic, S. Ling, J.S. Camp, Advances, updates, and analytics for the computation-ready, experimental metal–organic framework database: CoRE MOF 2019, J. Chem. Eng. 64 (2019) 5985–5998, https://doi.org/10.1021/acs.jced.9b00835.
[28] D. Dubbeldam, S. Calero, D.E. Ellis, R.Q. Snurr, RASPA: Molecular simulation software for adsorption and diffusion in flexible nanoporous materials, Mol. Simul. 42 (2016) 81–101, https://doi.org/10.1080/08927022.2015.1010082.
[29] A.K. Rappé, C.J. Casewit, K. Colwell, W. Goddard Iii, W. Skiff, UFF, a full periodic table force field for molecular mechanics and molecular dynamics simulations, J. Am. Chem. Soc., 114 (1992) 10024-10035, 10.1021/ja00051a040.
[30] H. Demir, J.A. Greathouse, C.L. Staiger, J.J. Perry IV, M.D. Allendorf, D.S. Sholl, DFT-based force field development for noble gas adsorption in metal organic frameworks, J. Mater. Chem. A 3 (2015) 23539–23548, https://doi.org/10.1039/C5TA06201B.
[31] T. Watanabe, D.S. Sholl, Accelerating applications of metal–organic frameworks for gas adsorption and separation by computational screening of materials, Langmuir 28 (2012) 14114–14128, https://doi.org/10.1021/la301915s.
[32] O.K. Farha, A.Ö. Yazaydın, I. Eryazici, C.D. Malliakas, B.G. Hauser, M. G. Kanatzidis, S.T. Nguyen, R.Q. Snurr, J.T. Hupp, De novo synthesis of a metal–organic framework material featuring ultrahigh surface area and gas storage capacities, Nat. Chem. 2 (2010) 944–948, https://doi.org/10.1038/nchem.834.
[33] J. Liu, J.T. Culp, S. Natesakhawat, B.C. Bockrath, B. Zande, S. Sankar, G. Garberoglio, J.K. Johnson, Experimental and theoretical studies of gas adsorption in $Cu_3(BTC)_2$: an effective activation procedure, J. Phys. Chem. C 111 (2007) 9305–9313, https://doi.org/10.1021/jp071449i.
[34] E. Pantatosaki, G.K. Papadopoulos, On the computation of long-range interactions in fluids under confinement: Application to pore systems with various types of spatial periodicity, J. Chem. Phys. 127 (2007), 164723, https://doi.org/10.1063/1.2799986.
[35] J. Pérez-Pellitero, H. Amrouche, F.R. Siperstein, G. Pirngruber, C. Nieto-Draghi, G. Chaplais, A. Simon-Masseron, D. Bazer-Bachi, D. Peralta, N. Bats, Adsorption of CO_2, CH_4, and N_2 on zeolitic imidazolate frameworks: experiments and simulations, Chem. Eur. J 16 (2010) 1560–1571, https://doi.org/10.1002/chem.200902144.
[36] A.L. Dzubak, L.-C. Lin, J. Kim, J.A. Swisher, R. Poloni, S.N. Maximoff, B. Smit, L. Gagliardi, Ab initio carbon capture in open-site metal–organic frameworks, Nat. Chem. 4 (2012) 810–816, https://doi.org/10.1038/nchem.1432.
[37] J.G. McDaniel, S. Li, E. Tylianakis, R.Q. Snurr, J. Schmidt, Evaluation of force field performance for high-throughput screening of gas uptake in metal–organic frameworks, J. Phys. Chem. C 119 (2015) 3143–3152, https://doi.org/10.1021/jp511674w.
[38] C.E. Wilmer, R.Q. Snurr, Towards rapid computational screening of metal-organic frameworks for carbon dioxide capture: Calculation of framework charges via charge equilibration, Chem. Eng. J. 171 (2011) 775–781, https://doi.org/10.1016/j.cej.2010.10.035.
[39] P.P. Ewald, Die berechnung optischer und elektrostatischer gitterpotentiale, Ann. Phys. 369 (1921) 253–287, https://doi.org/10.1002/andp.19213690304.
[40] M.G. Martin, J.I. Siepmann, Transferable potentials for phase equilibria. 1. united-atom description of n-alkanes, J. Phys. Chem. B, 102 (1998) 2569-2577, 10.1021/jp972543.
[41] V. Buch, Path integral simulations of mixed para-D2 and ortho-D2 clusters: The orientational effects, J. Chem. Phys. 100 (1994) 7610–7629, https://doi.org/10.1063/1.466854.
[42] C. Mellot, J. Lignieres, Monte carlo simulations of N_2 and O_2 adsorption in silicalite and CaLSX zeolites, Mol. Simul. 18 (1997) 349–365, https://doi.org/10.1080/08927029708024130.
[43] K. Makrodimitris, G.K. Papadopoulos, D.N. Theodorou, Prediction of permeation properties of CO_2 and N_2 through silicalite via molecular simulations, J. Phys. Chem. B 105 (2001) 777–788, https://doi.org/10.1021/jp002866x.
[44] J.J. Potoff, J.I. Siepmann, Vapor–liquid equilibria of mixtures containing alkanes, carbon dioxide, and nitrogen, AIChE J. 47 (2001) 1676–1682, https://doi.org/10.1002/aic.690470719.
[45] H. Daglar, S. Keskin, Computational screening of metal–organic frameworks for membrane-based $CO_2/N_2/H_2O$ Separations: Best materials for flue gas separation, J. Phys. Chem. C 122 (2018) 17347–17357, https://doi.org/10.1021/acs.jpcc.8b05416.
[46] S. Nosé, A unified formulation of the constant temperature molecular dynamics methods, J. Chem. Phys. 81 (1984) 511–519, https://doi.org/10.1063/1.447334.
[47] S. Keskin, D.S. Sholl, Selecting metal organic frameworks as enabling materials in mixed matrix membranes for high efficiency natural gas purification, Energy Environ. Sci. 3 (2010) 343–351, https://doi.org/10.1039/B923980B.
[48] J.C. Maxwell, Electricity and magnetism, Dover New York, 1954.
[49] G. Yilmaz, S. Keskin, Predicting the performance of zeolite imidazolate framework/polymer mixed matrix membranes for CO_2, CH_4, and H_2 separations using molecular simulations, Ind. Eng. Chem. Res. 51 (2012) 14218–14228, https://doi.org/10.1021/ie302290a.
[50] I. Erucar, S. Keskin, Screening metal–organic framework-based mixed-matrix membranes for CO_2/CH_4 separations, Ind. Eng. Chem. Res. 50 (2011) 12606–12616, https://doi.org/10.1021/ie201885s.
[51] C. Altintas, S. Keskin, Molecular simulations of porous coordination network-based mixed matrix membranes for CO_2/N_2 separations, Mol. Simul. 41 (2015) 1396–1408, https://doi.org/10.1080/08927022.2015.1028933.
[52] Y.-S. Bae, O.K. Farha, J.T. Hupp, R.Q. Snurr, Enhancement of CO_2/N_2 selectivity in a metal-organic framework by cavity modification, J. Mater. Chem. 19 (2009) 2131–2134, https://doi.org/10.1039/B900390H.
[53] H.C. Gulbalkan, Z.P. Haslak, C. Altintas, A. Uzun, S. Keskin, Assessing CH_4/N_2 separation potential of MOFs, COFs, IL/MOF, MOF/Polymer, and COF/Polymer composites, Chem. Eng. J. 428 (2022), 131239, https://doi.org/10.1016/j.cej.2021.131239.
[54] V. Smil, Natural gas: fuel for the 21st century, John Wiley & Sons, 2015.
[55] Z. Qiao, C. Peng, J. Zhou, J. Jiang, High-throughput computational screening of 137953 metal–organic frameworks for membrane separation of a $CO_2/N_2/CH_4$ mixture, J. Mater. Chem. A 4 (2016) 15904–15912, https://doi.org/10.1039/C6TA06262H.
[56] G. Avci, S. Velioglu, S. Keskin, High-throughput sreening of MOF adsorbents and membranes for H_2 purification and CO_2 capture, ACS Appl. Mater. Interfaces 10 (2018) 33693–33706, https://doi.org/10.1021/acsami.8b12746.
[57] Z. Qiao, K. Zhang, J. Jiang, In silico screening of 4764 computation-ready, experimental metal–organic frameworks for CO_2 separation, J. Mater. Chem. A 4 (2016) 2105–2114, https://doi.org/10.1039/C5TA08984K.
[58] H. Daglar, H.C. Gulbalkan, G. Avci, G.O. Aksu, O.F. Altundal, C. Altintas, I. Erucar, S. Keskin, Effect of metal–organic framework (MOF) database selection on the assessment of gas storage and separation potentials of MOFs, Angew. Chem. 133 (2021) 7907–7916, https://doi.org/10.1002/anie.202015250.
[59] J. Huang, J. Zou, W.W. Ho, Carbon dioxide capture using a CO_2-selective facilitated transport membrane, Ind. Eng. Chem. Res. 47 (2008) 1261–1267, https://doi.org/10.1021/ie070794r.
[60] T.N. Veziroglu, 21st Century's energy: Hydrogen energy system, in: Assessment of hydrogen energy for sustainable development, Springer, 2007, pp. 9-31.
[61] M. Yáñez, A. Ortiz, D. Gorri, I. Ortiz, Comparative performance of commercial polymeric membranes in the recovery of industrial hydrogen waste gas streams, Int. J. Hydrogen Energy 46 (2021) 17507–17521, https://doi.org/10.1016/j.ijhydene.2020.04.026.
[62] C.A. Scholes, U.K. Ghosh, Review of membranes for helium separation and purification, Membranes 7 (2017) 9, https://doi.org/10.3390/membranes7010009.
[63] J. Sunarso, S.S. Hashim, Y. Lin, S. Liu, Membranes for helium recovery: An overview on the context, materials and future directions, Sep. Purif. Technol. 176 (2017) 335–383, https://doi.org/10.1016/j.seppur.2016.12.020.
[64] M.A. Carreon, S. Li, J.L. Falconer, R.D. Noble, Alumina-supported SAPO-34 membranes for CO_2/CH_4 separation, J. Am. Chem. Soc. 130 (2008) 5412–5413, https://doi.org/10.1021/ja801294f.
[65] S. Denning, J. Lucero, C.A. Koh, M.A. Carreon, Chabazite zeolite SAPO-34 membranes for He/CH_4 separation, ACS Mater. Lett. 1 (2019) 655–659, https://doi.org/10.1021/acsmaterialslett.9b00324.
[66] R. Krishna, J.M. van Baten, In silico screening of zeolite membranes for CO_2 capture, J. Membr. Sci. 360 (2010) 323–333, https://doi.org/10.1016/j.memsci.2010.05.032.
[67] B.D. Freeman, Basis of permeability/selectivity tradeoff relations in polymeric gas separation membranes, Macromolecules 32 (1999) 375–380, https://doi.org/10.1021/ma9814548.
[68] F. Salles, D.I. Kolokolov, H. Jobic, G. Maurin, P.L. Llewellyn, T. Devic, C. Serre, G. Ferey, Adsorption and diffusion of H_2 in the MOF type systems MIL-47 (V) and MIL-53 (Cr): a combination of microcalorimetry and QENS experiments with molecular simulations, J. Phys. Chem. C 113 (2009) 7802–7812, https://doi.org/10.1021/jp811190g.
[69] F. Salles, A. Ghoufi, G. Maurin, R.G. Bell, C. Mellot-Draznieks, G. Férey, Molecular dynamics simulations of breathing MOFs: Structural transformations of MIL-53 (Cr) upon thermal activation and CO_2 adsorption, Angew. Chem. Int. Ed. 47 (2008) 8487–8491, https://doi.org/10.1002/anie.200803067.
[70] M.V. Parkes, H. Demir, S.L. Teich-McGoldrick, D.S. Sholl, J.A. Greathouse, M. D. Allendorf, Molecular dynamics simulation of framework flexibility effects on noble gas diffusion in HKUST-1 and ZIF-8, Micropor. Mesopor. Mat. 194 (2014) 190–199, https://doi.org/10.1016/j.micromeso.2014.03.027.
[71] J.A. Gee, J. Chung, S. Nair, D.S. Sholl, Adsorption and diffusion of small alcohols in zeolitic imidazolate frameworks ZIF-8 and ZIF-90, J. Phys. Chem. C 117 (2013) 3169–3176, https://doi.org/10.1021/jp312489w.
[72] E. Haldoupis, T. Watanabe, S. Nair, D.S. Sholl, Quantifying large effects of framework flexibility on diffusion in MOFs: CH_4 and CO_2 in ZIF-8, ChemPhysChem 13 (2012) 3449–3452, https://doi.org/10.1002/cphc.201200529.
[73] E. Haldoupis, S. Nair, D.S. Sholl, Efficient calculation of diffusion limitations in metal organic framework materials: A tool for identifying materials for kinetic separations, J. Am. Chem. Soc. 132 (2010) 7528–7539, https://doi.org/10.1021/ja1023699.
[74] I. Erucar, S. Keskin, Computational modeling of bio-MOFs for CO_2/CH_4 separations, Chem. Eng. Sci. 130 (2015) 120–128, https://doi.org/10.1016/j.ces.2015.03.016.

[75] I. Erucar, S. Keskin, Computational assessment of MOF membranes for CH_4/H_2 separations, J. Membr. Sci. 514 (2016) 313–321, https://doi.org/10.1016/j.memsci.2016.04.070.
[76] A. Ozcan, R. Semino, G. Maurin, A.O. Yazaydin, Modeling of gas transport through polymer/MOF interfaces: A microsecond-scale concentration gradient-driven molecular dynamics study, Chem. Mater. 32 (2020) 1288–1296, https://doi.org/10.1021/acs.chemmater.9b04907.
[77] J. Winarta, A. Meshram, F. Zhu, R. Li, H. Jafar, K. Parmar, J. Liu, B. Mu, Metal–organic framework-based mixed-matrix membranes for gas separation: An overview, J. Polym Sci. 58 (2020) 2518–2546, https://doi.org/10.1002/pol.20200122.